the plant journal

SEB SOCIETY FOR EXPERIMENTAL BIOLOGY

The Plant Journal (2026) **126,** e70913 doi: 10.1111/tpj.70913

FOCUSED REVIEW

Architectural and biochemical advances in understanding microbial CO_2 concentrating mechanisms

Cornelia E. M. Flothow and Andreas M. Küffner*

Max Planck Institute for Multidisciplinary Sciences, Am Faßberg 11, Göttingen 37077, Lower Saxony, Germany

Received 3 November 2025; revised 2 April 2026; accepted 24 April 2026.
*For correspondence (e-mail andreas.kueffner@mpinat.mpg.de).

SUMMARY

CO_2 concentrating mechanisms (CCMs) are ubiquitous in phototrophs. They are found in the micro as well as the macro world. Different domains of life have developed strikingly different approaches to concentrate inorganic carbon around Rubisco, the most prevalent enzyme on earth. While prokaryotes have developed carboxysomes, icosahedral shell protein cages, microbial eukaryotic phototrophs such as green algae, on the other hand, have developed pyrenoids, liquid–liquid phase separated organelles. In contrast to carboxysomes and pyrenoids, which represent biophysical CCMs, some vascular plants (C4 & CAM plants) have developed biochemical ways of concentrating CO_2 around Rubisco. In this review, we discuss advances in structural, biochemical, and mechanistic understanding of microbial CCMs in the last 5–10 years.

Keywords: carbonate transporters, carboxysomes, CO_2 concentrating mechanisms, CO_2 fixation, microbial organelles, one-carbon metabolism, photosynthesis, pyrenoids, Rubisco.

INTRODUCTION

CO_2 concentrating mechanisms (CCMs) represent one of the most innovative evolutionary solutions enabling autotrophic organisms to thrive despite fluctuating and often limiting environmental CO_2 levels. CCMs are composed of integrated biochemical and structural adaptations, which enhance CO_2 supply to the central Calvin–Benson–Bassham (CBB) cycle carboxylase Rubisco. Hence, CCMs overcome Rubisco's relatively low selectivity and catalytic rate (de Pins et al., 2025), which is specifically relevant in environments where dissolved CO_2 is scarce.

The earliest evidence for CCMs arose from physiological studies in the mid-20th century that observed unexpectedly high rates of photosynthesis and low rates of photorespiration in land plants. The C4 photosynthetic pathway, first proposed by Kortschak, Hatch, and Slack in the 1960s, was a major breakthrough (Hatch & Slack, 1966; Iglesias et al., 1987; Kortschak et al., 1965). It explained how specialized leaf anatomy and biochemical partitioning allow many terrestrial plants to pre-concentrate CO_2 around Rubisco, thus greatly improving efficiency under warm, dry conditions. The concept of the 'CO_2 pump' subsequently surfaced in studies of aquatic microorganisms, where biochemical shuttles and cellular structures were hypothesized to elevate CO_2 levels at the carboxylation sites (Kaplan & Reinhold, 1999; Rae et al., 2013; Shively, Ball, Brown, & Saunders, 1973).

The finding of CCMs in prokaryotic cyanobacteria and eukaryotic algae marked another milestone for understanding the most prevalent one-carbon metabolism. In cyanobacteria, membrane transporters for inorganic carbon (C_i; bicarbonate and CO_2) and highly ordered protein microcompartments termed carboxysomes were discovered (Gantt & Conti, 1969). These structures encapsulate Rubisco together with a carbonic anhydrase (CA) and act as biophysical CCMs, creating microenvironments with locally elevated CO_2 concentrations (Price & Badger, 1989a; Shively, Ball, & Kline, 1973; So et al., 2004). Meanwhile, most algae (i.e., green algae, red algae, diatoms, some dinoflagellates, haptophytes, cryptophytes, chlorarachniophytes, euglenids as well as a few brown algae and glaucophytes) and most hornwort species were shown to organize Rubisco into a distinct organelle known as the pyrenoid (Barrett et al., 2021). These organelles are coupled to thylakoid tubules that deliver CO_2 generated by nearby CAs and can additionally be surrounded by a starch sheath or other encompassing barriers (Freeman Rosenzweig et al., 2017; Lacoste-Royal & Gibbs, 1987; Mackinder et al., 2016; Ohad et al., 1967; Sager & Palade, 1957).

© 2026 The Author(s).
The Plant Journal published by Society for Experimental Biology and John Wiley & Sons Ltd.
This is an open access article under the terms of the Creative Commons Attribution License, which permits use, distribution and reproduction in any medium, provided the original work is properly cited.

Molecular genetics in the late 20th and early 21st century enabled the identification and functional dissection of the many genes involved in CCM regulation (Price et al., 2008). Key discoveries included the transport proteins BicA and SbtA in cyanobacteria and the scaffolding protein Essential Pyrenoid Component 1 (EPYC1) in *Chlamydomonas*, which links Rubisco molecules to form pyrenoid matrices (Mackinder et al., 2016; Shibata et al., 2001). Genomic studies provided vital insights into CCM diversity across microbial lineages, revealing that carboxysome and pyrenoid-like structures evolved multiple times, presumably in response to falling atmospheric CO_2 levels throughout Earth's history (Flamholz & Shih, 2020; Long et al., 2024; Melnicki et al., 2021; Moromizato et al., 2024; Rae et al., 2013; Sandrini et al., 2014; Sommer et al., 2017; Villarreal & Renner, 2012; Whitehead et al., 2014).

While these organelles have been known for decades, the last two have seen remarkable progress in understanding the biochemical and structural mechanisms underpinning CCMs. Cryo-electron tomography (cryo-ET), proteomics, and live cell imaging have mapped the 3D organization of carboxysomes and pyrenoids with high resolution, revealing how phase separation, specialized shell proteins, and dynamic protein–protein interactions coordinate Rubisco packaging and catalytic activity (Engel et al., 2015; Freeman Rosenzweig et al., 2017; Huang et al., 2020; Ni et al., 2022; Wunder et al., 2018; Zhan et al., 2018). These technological advances revealed that CCM microcompartments operate as liquid-like droplets or crystalline matrices, and how CA strategically converts bicarbonate to CO_2 in close proximity to the active site of Rubisco (Blikstad et al., 2023; Meyer & Griffiths, 2013; Zang et al., 2021).

Biochemical reconstitution and synthetic biology have further illuminated CCM function by enabling the assembly of carboxysome and pyrenoid proteins in heterologous model systems, such as *Escherichia coli* or plant chloroplasts, respectively (Atkinson et al., 2016; Flamholz et al., 2020). By transplanting the CCM, it was possible to demonstrate its mechanistic sufficiency for conferring growth under ambient air and the required components for functionality, including specialized linkers and shell proteins, have been elucidated. Parallel work in plant biology explored the introduction of cyanobacterial and proteobacterial CCMs into C3 crops, with the aim of enhancing photosynthetic rates in order to increase crop yields in global agriculture (Chen et al., 2023; Hanson et al., 2016).

The *de novo* assembly, transplantation, and redesign of CCM components continue to be a primary focus for current research (Chen et al., 2023; Sun, Chen, et al., 2025; Trettel et al., 2025). Recent works have not only engineered carboxysomes in plant chloroplasts, but also manipulated the Rubisco-binding modes of scaffold proteins, and optimized shell permeability for selective metabolite flux. Sophisticated genetic toolkits now allow for rapid construction, testing, and evolutionary improvement of CCM modules (Hennacy & Jonikas, 2020; Trettel et al., 2025).

In summary, understanding and engineering CCMs spans a broad spectrum of fields such as plant physiology, evolutionary biology, molecular genetics, and high-resolution structural biochemistry. While early physiological puzzles revealed distinct solutions (i.e., carboxysomes versus pyrenoids) to Rubisco's shortcomings, each of them represents a blueprint for next-generation carbon-fixation engineering. Even though carboxysomes and pyrenoids have been discovered almost 75 years ago, CCM research remains a frontier, at the intersection of biology and biotechnology, for understanding how a putatively inefficient CO_2 assimilating cycle (CBB cycle) became the most prevalent cycle on Earth (Fuchs, 2011; Liang et al., 2020).

CARBOXYSOMES—THE DICE-LIKE MARVELS FOR CONCENTRATING CO_2

Structural studies using cryo-EM and cryo-ET elucidate the architecture and mechanism of carboxysomes

In the past decade, unprecedented advances in structural biology have illuminated the architecture and assembly principles of carboxysomes. Using single-particle cryo-electron microscopy (cryo-EM), cryo-ET, and atomic force microscopy (AFM), near atomic-scale details of shell protein matrices, Rubisco encapsulation, assembly intermediates, and permeability properties have been resolved (Evans et al., 2023; Huang et al., 2022; Kong et al., 2024; Sarkar et al., 2024; Sutter et al., 2019).

Carboxysomes are protein microcompartments built from thousands of proteins that form an icosahedral structure that is similar to cage shaped virus capsids (Kerfeld et al., 2005; Tanaka et al., 2008). High-resolution cryo-EM analysis has revealed that both α- and β-carboxysomes possess shells composed of two main protein types: hexamer-forming proteins (BMC domain-containing, for example, α-carboxysomes: CsoS1A-C; β-carboxysomes: CcmK2/CcmK4) and pentamer-forming proteins (CsoS4/CcmL) (Ni et al., 2022; Sarkar et al., 2024). The hexamers tile the majority of the shell surface, forming 20 triangular facets that create semi-permeable barriers, while the pentamers cap the 12 vertices of the icosahedron. The orientation of hexamer and pentamer, as well as their intermolecular contacts, define the shell's selectivity and mechanical stability (Sutter et al., 2019).

In native α-carboxysomes (Figure 1a), the hexamers form pores at their central axes, which facilitate controlled molecular transit, and are further joined by pseudohexameric proteins, such as CsoS1D, that are presumed to act as gated conduits for the transport of ribulose-1,5-bisphosphate (RuBP) and other larger metabolites via

© 2026 The Author(s).

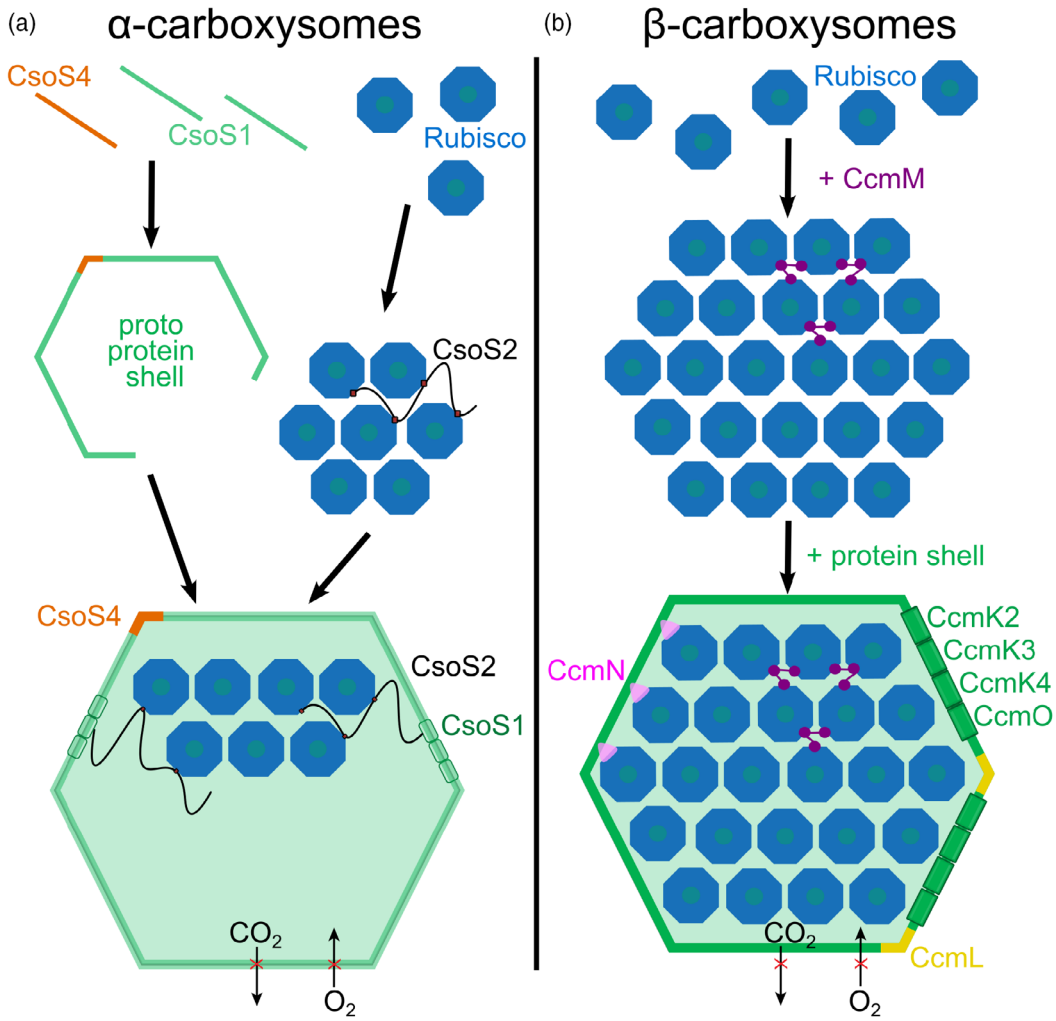


Figure 1. The assembly pathway of α- and β-carboxysomes.
(a) The shell and cargo of α-carboxysomes can assemble concurrently. The Rubisco assembly formation is facilitated by the intrinsically disordered linker protein CsoS2, and the protein shell is composed of hexamer proteins CsoS1 and pentamer proteins CsoS4. CsoS4 also forms pores enabling molecular transit through the shell.
(b) In contrast, β-carboxysome assembly follows a 'core first, shell second' mechanism, beginning with Rubisco packing facilitated through the scaffolding protein CcmM. When the microcompartment reaches a critical size, CcmN mediates the interaction with the shell proteins CcmK2, CcmK3, CcmK4, CcmO (hexamers) and CcmL (pentamer).

stacked trimers forming an airlock. Additionally, subtle charge differences in CsoS1A versus CsoS1C hexamers result in variable selectivity for negatively charged metabolites. Via shell protein mutations and engineered variants, this permeability has been experimentally modulated (Li et al., 2020; Sun et al., 2022; Wang et al., 2024; Huang et al., 2022; Faulkner et al., 2020).

Inside the α-carboxysome, the intrinsically disordered protein (IDP) CsoS2 determines architecture and assembly dynamics. CsoS2 contains multiple tandem repeat domains in its N-terminal region, each capable of binding to a conserved surface of the Rubisco holoenzyme by engaging specific acidic and hydrophobic residues on Rubisco's large and small subunits (Blikstad et al., 2023; Ni et al., 2022, 2023; Oltrogge et al., 2020; Turnšek et al., 2024). This positions Rubisco in a tight matrix or array formation within the lumen of the carboxysome. Structural and mutational studies have shown that around 10–13 CsoS2 repeats (four N-terminal, six middle region, three C-terminal in *Halothiobacillus neapolitanus*) per linker may be present, each acting as a modular tether (Cai et al., 2015; Ni et al., 2023; Oltrogge et al., 2020). Both repeat number and post-translational modifications finely regulate the affinity of interaction. Simultaneously, the C-terminal region of CsoS2 interacts with the inner facets of the shell proteins, specifically conserved grooves on CsoS1 (hexamers) and CsoS4 (pentamers), through conserved [I/V]TG motifs which dock precisely into the

© 2026 The Author(s).

threefold junctions between CsoS1As and CsoS1A/CsoS4A interfaces. This docking is mediated by hydrogen bonds ([I/V]TG → CsoS1A H79, CsoS2 R855 → CsoS4A H21) and salt bridges (CsoS2 R731 → CsoS4A E22, CsoS2 R784 → CsoS4A E69), which effectively anchor the Rubisco condensate to discrete locations on the shell (Ni et al., 2023; Oltrogge et al., 2024).

The pairwise coordination between Rubisco subunits and the CsoS2 repeats forms local enzyme clusters, which yield a higher-order concentric organization into several layers, as visualized by cryo-ET (Ni et al., 2022). This layering generates structurally distinct zones within the carboxysome that may influence substrate channeling and metabolic flux. The spatial proximity enforced by CsoS2 is argued to accelerate the delivery of CO_2 produced by the shell-localized CA to Rubisco's active sites.

Biophysical experiments based on *in vitro* reconstitution systems with Rubisco and an N-terminal fragment of CsoS2 have demonstrated that the resulting Rubisco-CsoS2 condensate exhibits properties of a liquid-like phase (Oltrogge et al., 2020), marked by rapid molecular exchange and dynamic rearrangement, which could be crucial for organelle repair, turnover, and adaptability in response to changing cellular CO_2 levels as hypothesized for pyrenoids (Freeman Rosenzweig et al., 2017; Hill et al., 2020; Huffine et al., 2024; Niederhuber et al., 2017; Zang et al., 2021). Remarkably, this condensate can self-assemble independently of the shell structure: purified CsoS2 and Rubisco spontaneously form dense condensates, while shell protein mixtures can assemble into hollow capsids under physiological conditions in the absence of cargo. These findings illustrate the inherent modularity and self-sufficiency of the matrix and the shell (Figure 1a) (Menon et al., 2008; Oltrogge et al., 2024; Wang et al., 2024).

In vivo and synthetic systems have further revealed that fusion of additional M-regions, or mutation of CsoS2 domains, can dramatically alter carboxysome size, cargo density, and permeability, providing evidence for a tunable assembly process driven by the scaffold's sequence and structure (Li et al., 2024; Long et al., 2018; Oltrogge et al., 2024).

In contrast to α-carboxysomes, β-carboxysome biogenesis proceeds via a step-wise assembly (Figure 1b), in which Rubisco packing and microcompartment construction are directed by the scaffold protein CcmM. CcmM's two isoforms, M58 and M35, which are produced through alternative translation initiation, contain multiple small subunit-like (SSUL) domains that are homologous to Rubisco's small subunit, as well as a C-terminal γ-CA domain in M58 (Ryan et al., 2019). These SSUL domains promote the nucleation and organization of Rubisco into tightly packed, paracrystalline arrays that exhibit pseudo-hexagonal symmetry in the core of the carboxysomes (Sun, Sheng, et al., 2025). Each CcmM molecule can simultaneously bind several Rubiscos, aligning them in near-hexagonally packed arrays that maximize Rubisco concentration (Kong et al., 2024).

After Rubisco assemblies reach a critical size, the encapsulation machinery is recruited. CcmN contains a unique linker peptide at its C-terminus (~17–18 amino acids forming an amphipathic α-helix) that mediates the interaction between the Rubisco-CcmM matrix and the following shell proteins: CcmK2, CcmK3, CcmK4, CcmL, and CcmO (Kinney et al., 2012; Lin et al., 2014; Sun et al., 2021). The shell proteins self-assemble around these pre-formed cores facilitated by CcmN, resulting in the canonical icosahedral morphology but with variable facet composition (i.e., stoichiometry of paralogs) depending on organism and environmental signals (Figure 1b). While the α-carboxysome shell and cargo assemble concurrently, β-carboxysomes rely on this 'core first, shell second' mechanism, such that empty shells rarely form (Cameron et al., 2013; Sutter et al., 2019).

On a nanoscale, β-carboxysomes can reach diameters of 100–400 nm, dwarfing their α-carboxysome counterparts, which typically range from 40 (engineered) to 160 nm (Oltrogge et al., 2024). This larger size is attributed to the capacity for the formation of large Rubisco clusters through CcmM and the shell not being able to self-assemble (Whitehead et al., 2014). Thus, β-carboxysomes can contain ~1.5 times more Rubisco complexes compared to α-carboxysomes (Whitehead et al., 2014; Sun et al., 2022; Faulkner et al., 2017; Ni et al., 2022; Niederhuber et al., 2017; Sun, Sheng, et al., 2025).

Carboxysomes, while unique in their CO_2 concentrating function, share core architectural principles with other bacterial microcompartments (BMCs), such as propanediol utilization BMC, ethanolamine utilization BMC, or glycyl radical enzyme-containing BMC. Comparative studies show conservation in BMC hexamer and pentamer motifs, permeability determinants, and shell formation strategies (Li et al., 2021; Ochoa et al., 2021; Raza et al., 2024; Sutter et al., 2021; Trettel et al., 2023; Young et al., 2025).

Biochemical characterization of catalytic mechanism

The selectively permeable shell of carboxysomes creates a microenvironment that concentrates CO_2 near Rubisco's active site while minimizing the competing oxygenation reaction that leads to photorespiration (Faulkner et al., 2020; Sarkar et al., 2024). The fundamental principle underlying carboxysome function involves the uptake of bicarbonate (HCO_3^-) from the cytoplasm through pores in the shell. This process utilizes the 50–1000-fold approximate up-concentration of bicarbonate in the cytosol compared to the environment and, thus, yields a saturated inner lumen of the carboxysomes (Flamholz et al., 2020; Huang et al., 2022).

© 2026 The Author(s).

Inside the carboxysome, CA catalyzes the rapid conversion of HCO_3^- to CO_2 and H_2O, generating local CO_2 concentrations that can be 10–100 times above ambient levels (Mangan & Brenner, 2014). This enables Rubisco to operate near its maximum carboxylation rate with minimized oxygenation activity (Flamholz et al., 2022; Long et al., 2018; Mangan & Brenner, 2014). The specific protein–protein interactions between disordered regions and Rubisco creates enzyme supercomplexes that presumably optimize substrate channeling and catalytic efficiency (Blikstad et al., 2023). In α-carboxysomes of *Cyanobium* the CA CsoSCA, unlike the CA from the chemoautotrophic bacterium *H. neapolitanus*, displays additional allosteric activation by RuBP, which suggests a sophisticated regulatory mechanism that coordinates the activities of both enzymes (CA & Rubisco) within the carboxysome microenvironment (Pulsford et al., 2024).

On the edge of the carboxysome, the shell proteins create pores with selective permeability for charged metabolites such as HCO_3^- and 3-phosphoglycerate. Mathematical modeling and experimental studies have demonstrated that optimal carboxysome function requires fine-tuned and rapid HCO_3^- influx while minimizing CO_2 leakage (Faulkner et al., 2020; Huang et al., 2022; Mahinthichaichan et al., 2018). Recent evidence, however, also suggests that CO_2 retention rather than selective exclusion of oxygen may be the primary mechanism for CCM efficiency (Mangan et al., 2016). *In vivo* biochemical investigations of carboxysome function have shown that CA activity must be strictly compartmentalized within the carboxysome, as cytosolic expression of CA destroys CCM function by dissipating the bicarbonate gradient before it can be utilized for CO_2 up-concentration (Flamholz et al., 2020, 2022; Price & Badger, 1989b).

Beyond the shell, the apparent catalytic parameters of encapsulated Rubisco appear to differ significantly from those of the free enzyme. Experimental studies have demonstrated that carboxysome-encapsulated Rubisco exhibits approximately twofold higher apparent Michaelis–Menten constants for RuBP compared to the free enzyme, with K_M values increasing from approximately 36 ± 1 μM for free Rubisco to 59 ± 3 μM for the carboxysome-encapsulated Rubisco (Long et al., 2018). This indicates that the proteinaceous shell creates a diffusional barrier that restricts RuBP access to the enzyme's active site. This elevated K_M for RuBP has been observed in α-carboxysomes isolated from native cyanobacteria, as well as those reconstituted in transgenic plants and is suggested to be consistent across both α- and β-carboxysomes, suggesting a fundamental consequence of encapsulation rather than species-specific effects (Long et al., 2018, 2021; Orr et al., 2020; Whitehead et al., 2014). Restricted substrate access appears to result from the selective permeability properties of the shell proteins, particularly the hexameric BMC domain-containing proteins. These accommodate the passage of the bulkier RuBP molecule through channels, which also must restrict the efflux of CO_2. Molecular dynamics simulations suggest that RuBP exhibits the slowest permeability coefficient among all CBB cycle intermediates tested, with permeability values approximately 10-fold lower than smaller metabolites such as 3-phosphoglycerate (Long et al., 2021; Rae et al., 2013). It appears that the three-dimensional structure and charge distribution of RuBP creates significant energetic barriers for transit through the shell pores. In contrast to the restricted RuBP kinetics, the authors state that carboxysome-encapsulated Rubisco displays CO_2 kinetics that are remarkably similar to those of the free enzyme, with $K_M(CO_2)$ values (Michaelis–Menten constants for CO_2) remaining largely unchanged upon encapsulation (around 250 μM at standard atmosphere) (Long et al., 2018; Sarkar et al., 2024).

The authors further argue that the preservation of $K_M(CO_2)$ suggests for the carboxysome shell not to significantly impede CO_2 diffusion, consistent with molecular simulations showing that CO_2 has one of the highest permeability coefficients across the shell ($\sim 10^{-2}$ cm s^{-1}). This stands in contrast to its presumed role as a diffusional barrier for CO_2 (Faulkner et al., 2020; Sarkar et al., 2024). Furthermore, the turnover number (k_{cat}) of encapsulated Rubisco shows similar to slightly elevated catalytic rates despite the confinement, indicating that the high local enzyme concentration may partially compensate for reduced substrate accessibility. It is not clear if the CO_2/O_2 specificity factor ($S_{C/O}$) of encapsulated Rubisco generally remains similar to that of the free enzyme (Long et al., 2018; Sarkar et al., 2024). In theory, the apparent specificity should differ from the free enzyme because the elevated CO_2 concentrations achieved inside should effectively suppress oxygenation activity by mass action according to the current biochemical model. Computational modeling efforts suggest this theory by estimating a changed apparent $S_{C/O}$, showing dramatically enhanced carboxylation efficiency under physiological conditions with over 2600 CO_2 molecules fixed for every molecule that escapes the compartment (Sarkar et al., 2024).

Beyond the canonical mechanism of carboxysomes, they display a remarkable diversity as evidenced by the recently identified iota-class CAs (iCA) in sulfur-oxidizing bacteria. This CA does not require a metal cofactor in the reaction center but relies solely on the protein structure (Wieschollek et al., 2024; Yadav et al., 2024). Additionally, systems-level analysis indicates that carboxysomes may function as part of a larger cellular metabolon. In this metabolon, physically associated enzymes facilitate metabolite channeling and enhance carbon flux through the CBB cycle, with the carboxysome serving as a central hub that coordinates multiple metabolic pathways involved in CO_2 fixation (Abernathy et al., 2019; Huffine et al., 2023).

© 2026 The Author(s).

PYRENOIDS—THE MICROBIAL EUKARYOTIC SOLUTION FOR CONCENTRATING CO_2

Macro structure resolved by cryo-ET shows internal organization

Although most algae and hornwort species possess pyrenoids, they are not a mandatory feature. They come in a diverse set of organizations ranging from one to tens of pyrenoids per chloroplast and appear to be more structurally flexible than carboxysomes (Neofotis et al., 2021; Robison et al., 2025; Villarreal & Renner, 2012). They consist either of the pyrenoid matrix alone—a highly dense structure of Rubiscos—or of the matrix traversed by thylakoid membranes and can additionally be enveloped by a starch sheath or protein shell (Atkinson et al., 2024; Engel et al., 2015; He et al., 2023; Hennacy et al., 2024; Itakura et al., 2019; Nam et al., 2024). In the model green alga *Chlamydomonas reinhardtii*, pyrenoid constitution and assembly have been studied extensively, which has shown that Rubisco is first condensed by the IDP EPYC1 creating the pyrenoid matrix, which is then transversed by thylakoid tubules and finally enveloped by a starch sheath (Figure 2a). However, it has been observed that the pyrenoid architecture can vary significantly across species. For example, the model diatom *Phaeodactylum tricornutum* consists of a pyrenoid matrix that is transversed by only a single thylakoid tubule and is surrounded by a proteinaceous sheath of pyrenoid shell (PyShell) proteins, while hornworts such as *Anthoceros agrestis* are not transversed by thylakoid tubules but instead are surrounded by them. The red alga *Porphyridium cruentum* on the other hand exhibits a pyrenoid matrix transversed by a highly complex network of interconnected tubules without a surrounding sheath (Figure 2b) (Barrett et al., 2021; McKay & Gibbs, 1990; Robison et al., 2025; Shimakawa et al., 2024).

Inside the pyrenoid, Rubisco is tightly packed into hexagonal or cubic formations elucidated by cryo-ET studies of the *C. reinhardtii* pyrenoid (Engel et al., 2015). Using modified *in situ* cryo-ET and fluorescence recovery after photobleaching for ultrastructure elucidation of the pyrenoid, the formation of a liquid-like droplet was shown, marked by rapid molecular exchange and dynamic rearrangement (Freeman Rosenzweig et al., 2017). The mobility of the main protein constituents of the *C. reinhardtii* pyrenoid—Rubisco and the IDP EPYC1—further underpins the liquidity. This rapid exchange appears to be necessary for organelle repair, turnover, and response to changing cellular CO_2 levels (Freeman Rosenzweig et al., 2017). The prevalence of EPYC1 has also been demonstrated with proteomics, estimating that it is one of the most abundant proteins in the pyrenoid, playing a key role in the pyrenoid assembly (Mackinder et al., 2016, 2017; Wunder et al., 2018).

Unlike carboxysomes, in which a CA is located in the matrix, so that HCO_3^- is converted to CO_2 proximal to Rubisco, current evidence does not suggest a CA in the pyrenoid matrix (Fei et al., 2022). Instead, CAs are located in the lumen of thylakoid tubules that often spike into the pyrenoid matrix, or envelop it. These spiking or enveloping thylakoids show a remarkable range of diversity. The thylakoid sheets can surround the pyrenoid (i.e., in *A. agrestis* and some dinoflagellates), thylakoids can traverse the pyrenoid by forming a single disc that bisects the pyrenoid matrix (i.e., in *P. tricornutum* and several *Chlorella* species), or multiple non-connecting, parallel stacks of thylakoids can pass through the pyrenoid (common in green algae and *Euglena*; Figure 2) (Kusel-Fetzmann & Weidinger, 2008; Meyer et al., 2017; Treves et al., 2016). In *C. reinhardtii* the biogenesis of the spiking thylakoids is facilitated by SAGA1 on the matrix surface, followed by MITH1 drawing the membranes through the pyrenoid (Franklin et al., 2026; Hennacy et al., 2024). A suspected advantage of the segregation of Rubisco and the CA is that both enzymes can operate at their respective optimal pH levels (Fei et al., 2022; Robison et al., 2025).

Surrounding the pyrenoid, presumably to prevent CO_2 leakage, *C. reinhardtii* and many other algae lineages develop a starch sheath, which has been resolved through cryo-ET (Engel et al., 2015; Fei et al., 2025). Nonetheless, some pyrenoid-containing organisms do not feature such an envelope. Instead of starch sheaths, diatoms appear to use a protein shell (Nam et al., 2024; Shimakawa et al., 2024), while hornwort pyrenoids are surrounded by thylakoid stacks (Robison et al., 2025). It is not fully understood, if the starch sheath truly prevents the CO_2 leakage as is also disputed for the carboxysome shells, or if the enveloping structures have more architectural function as is suggested by the *saga1* mutant (Fei et al., 2025; Itakura et al., 2019).

Reverse genetic studies have further shown that not only a single pyrenoid but also many within one cell can be functional. For example, recent experiments have shown that *C. reinhardtii* cells that carry a mutation in the *SAGA1* gene have 10 pyrenoids on average. *C. reinhardtii* with the mutated *SAGA1* gene remains viable; however, as the mutation leads to a reduced photosynthetic efficiency, the mutant is only cultivatable in high CO_2 concentrations (Itakura et al., 2019). A naturally occurring example is the species *Scytosiphon lomentaria*. In this species, a second pyrenoid is formed *de novo* in the parental chloroplast prior to cell division, and subsequently the two pyrenoids are passed equally to the daughter cells upon division (Nagasato & Motomura, 2002). While most algae have only one pyrenoid, hornworts in general (i.e., *A. agrestis*) have multiple pyrenoids per chloroplast displaying considerable variation with ~25 pyrenoids observed in *Phaeoceros laevis* (Griffiths, 1970; Robison et al., 2025; Villarreal & Renner, 2012).

© 2026 The Author(s).

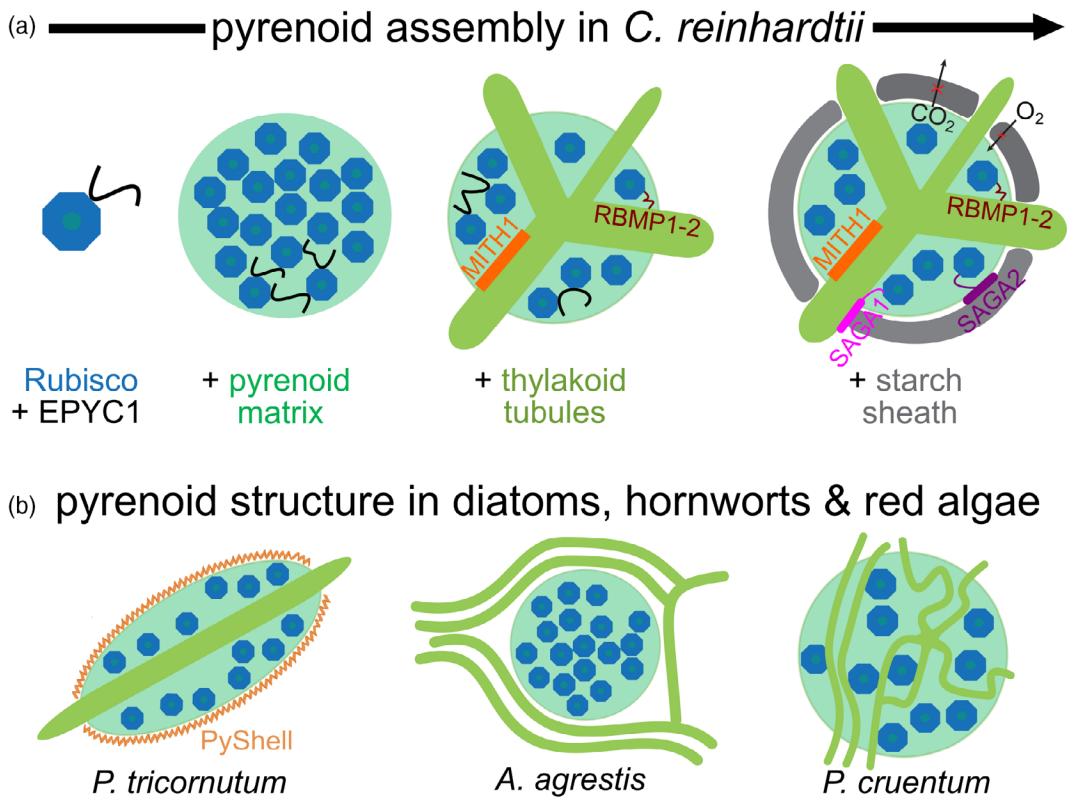


Figure 2. The architecture of pyrenoids in various species.
(a) The architecture and assembly pathway of pyrenoids in *Chlamydomonas reinhardtii*. Rubisco is aggregated by the intrinsically disordered protein EPYC1, creating a so-called pyrenoid matrix. In the next step, thylakoid tubules are drawn through the pyrenoid by MITH1, while RBMP1-2 mediates an interaction between the matrix and the thylakoid tubules. Finally, the pyrenoid is enveloped by a starch sheath. This process is facilitated by SAGA1 and SAGA2, which bind the starch plates and promote interaction between the matrix and the shell.
(b) Examples of different pyrenoid architectures occurring in the model diatom *Phaeodactylum tricornutum*, model hornwort *Anthoceros agrestis*, and red alga *Porphyridium cruentum*.

While the pyrenoid matrix is mainly constituted from Rubisco and EPYC1, and Rubisco specifically being the main protein observable with cryo-ET, proteomics studies of *C. reinhardtii* revealed that a total of 190 proteins are within the pyrenoid proteome (Zhan et al., 2018). Among the most abundant proteins in the *C. reinhardtii* proteome is Rubisco activase, which is often necessary for the continued activity of form I Rubiscos. This observation shows that similar to carboxysomes, in which Rubisco activases are at least suspected, the pyrenoid needs to sequester significant repair machineries to keep the organelle running (Sun et al., 2022). In contrast to green algae, the activase activity in non-green algae is taken on by the chaperone-like Rubisco activase CbbX (Mueller-Cajar et al., 2011; Kroth, 2015).

Even though *C. reinhardtii* has been studied most extensively, investigating other species has shown that the proteins involved in pyrenoid assembly may differ significantly from one species to another. While functional homologs to EPYC1 are also present in the genomes of other algae with pyrenoids, such as PYCO1 in diatoms (Oh et al., 2023) and CsLinker in chlorella (Barrett et al., 2024), they do not share any sequence homology. A recent study into the pyrenoid proteome of the chlorarachniophyte alga *Amorphochlora amoebiformis* identified the matrix protein PPAP28 as a potential Rubisco-binding linker protein. Since its homologs have not been detected in other chlorarachniophytes, the study suggested that PPAP28 is even species-specific (Moromizato et al., 2024). Such findings underline that the macro-structures of pyrenoids are highly diverse despite serving the same purpose and that even down to the individual protein homology can be minimal.

Reverse and forward genetics reveal the function of individual components

Using reverse and forward genetics, the functional components of pyrenoids in *C. reinhardtii*—the matrix, the shell and the tubules—have further been elucidated in recent years. These three essential CCM modules for the pyrenoid have been proposed based on phenotypic characterizations coupled to genetic deletions (for example the requirement for more ATP per CO_2 molecule fixed and/or a

© 2026 The Author(s).

diminished capacity to concentrate inorganic carbon) (Adler et al., 2022; Dao et al., 2025; Fei et al., 2022).

The first module represents a chloroplast CO_2 uptake system that uses either a stromal CA to facilitate the diffusive influx of CO_2 and conversion into HCO_3^- (i.e., the LCIB-dependent pathway) or an active pump to import HCO_3^- (i.e., HLA3/LCIA-mediated HCO_3^- uptake). The LCIB-dependent pathway is active under low CO_2 conditions, during which LCIB is dispersed throughout the chloroplast stroma. The mechanistic importance under low CO_2 conditions has been elucidated through *lcib* mutants (Δ*ad1*), which exhibit impaired photosynthesis and C_i transport (Duanmu et al., 2009; Wang & Spalding, 2014; Yamano et al., 2015).

The second module involves a system that transports HCO_3^- into the thylakoid lumen through channels in the thylakoid membrane, enabling HCO_3^- to diffuse into the tubules within the pyrenoid matrix, where it is converted back into CO_2 by a CA. The main channels for HCO_3^- transport from the chloroplast stroma to the thylakoid lumen are considered to be bestrophin-like proteins (BSTs), which are located on the thylakoid membrane. RNAi mutants with reduced expression of all three BST gene paralogous (BST1-3) were unable to survive under low CO_2 conditions (Mukherjee et al., 2019). BST4 has been proposed to be an additional HCO_3^- channel, with a particular importance during the transition from dark to light and for the regulation of the luminal pH in *C. reinhardtii* (Adler et al., 2023). Additionally, the importance of a CA (CAH3) has been demonstrated by the *Cah3* mutant, which exhibits impaired CCM function (Sinetova et al., 2012). The thylakoids transversing the pyrenoids are facilitated by SAGA1 on the matrix surface, followed by MITH1 drawing the membranes through the pyrenoid. Furthermore, Rubisco-Binding Membrane Proteins 1-2 (RBMP1-2) have been found to be essential by mediating interactions between the dense matrix and the thylakoid tubules (Adler et al., 2023; Meyer, Itakura, et al., 2020).

The third module represents a dense Rubisco core, that is, the pyrenoid matrix. This matrix is in the most studied pyrenoids formed through co-condensation of Rubisco with an associated liquid–liquid phase separation (LLPS) prone IDP. In *C. reinhardtii*, the essential function of EPYC1 in forming the pyrenoid matrix has been observed using fluorescence microscopy combined with reverse genetics, as *epyc1* mutants showed a misallocation of Rubisco, with a large fraction found outside the pyrenoid. This results in decreased CO_2 fixation through Rubisco, which explains the severe CCM defect observed in this mutant (He et al., 2020; Mackinder et al., 2016).

Pyrenoids are often surrounded by a defined physical barrier, which can be composed of starch plates (*C. reinhardtii*), a protein shell (diatoms) or thylakoid stacks. It has been hypothesized that this structure acts as a diffusional barrier to CO_2 and O_2. This effect has been supported by the *C. reinhardtii* mutant *sta2-1* that develops thinner starch plates due to a defective granule-bound starch synthase I and exhibits lower CCM efficiency at concentrations of CO_2 below ambient air (Toyokawa et al., 2020). Furthermore, the starch sheath appears to be involved in pyrenoid assembly, providing structural support (Atkinson et al., 2024; Barrett et al., 2021; Itakura et al., 2019). Several proteins have been identified as playing a role in the formation and maintenance of the starch sheath. Among these are SAGA1 and SAGA2 (Starch Granule Abnormal 1 and 2), which have been shown to bind to the starch plates and mediate interaction between the matrix and shell via a Rubisco-binding motif (He et al., 2023; Meyer, Itakura, et al., 2020). The variety of proteins observed to be involved in pyrenoid assembly, as determined through physiological and genetic experiments, supports the observation that pyrenoids evolved independently multiple times (Long et al., 2024; Moromizato et al., 2024).

In contrast to the reverse genetic experiments using knock-outs/knock-downs, transplantation efforts of the pyrenoid into plants have shown the extent as well as the limits of our understanding of pyrenoid function. While a considerable proportion of the CCM components of *C. reinhardtii* appear to be compatible with plants, at least regarding their appropriate localization (Atkinson et al., 2016), a fully functional pyrenoid has not yet been achieved in plant chloroplasts (Catherall et al., 2025). The first successful step was the expression of a proto-pyrenoid in the chloroplasts of *Arabidopsis thaliana*. This proto-pyrenoid consisted of EYPC1 and a plant–algal hybrid Rubisco (combining *A. thaliana* RbcL and *C. reinhardtii* RbcS). Using this engineered system, pyrenoid-like Rubisco condensation was observed (Atkinson et al., 2020). SAGA1 and SAGA2, responsible for recruiting starch around the pyrenoid matrix were successfully expressed in transgenic *A. thaliana* proto-pyrenoid lines which led to large, plate-like starch granules being observed around the edges of the matrix (Atkinson et al., 2024). The coexpression of MITH1 (Missing THylakoids 1) and SAGA1 in transgenic *A. thaliana* proto-pyrenoid lines successfully led to the formation of thylakoid membranes traversing through the proto-pyrenoid matrix (Catherall et al., 2025). However, their appearance was similar to plant thylakoid membranes, which suggests that there are still components involved in tubule formation and maturation that need to be identified.

In vitro reconstitution underpinning catalytic mechanism

Using enzymatic assays to assess the CO_2 fixation rates already show the effectiveness of minimal component pyrenoids. While recent studies have mostly focused on the *in vivo* formation and function of pyrenoids in *C. reinhardtii*, as well as their transplantation into plants, other

© 2026 The Author(s).

studies have examined the efficiency of *in vitro*-built minimal component pyrenoids, using a bottom-up approach (Küffner et al., 2024; Wunder et al., 2018). These minimal pyrenoids consist of a simple bacterial Rubisco, namely form II Rubisco from *Rhodospirillum rubrum*, and a *C. reinhardtii* EPYC1. Interestingly, only EPYC1 induced the formation of condensates compared to other LLPS-associated IDPs, emphasizing its role in pyrenoid assembly. Furthermore, Rubisco activity assays showed that the carboxylation rate of the Rubisco enzyme was significantly higher within the condensates compared to its rate when it was not phase separated. These results suggest that pyrenoids may have evolved from simple phase-separating Rubisco/EPYC1 complexes, which raises questions about the more complex assemblies and the evolution of modern pyrenoids.

The minimal bottom-up approach provides a blueprint for developing synthetic CO_2-concentrating organelles in plants using IDP-mediated phase separation principles. In addition, this approach can be employed to further develop pyrenoids consisting of EPYC1 and form I Rubiscos, such as RbcLS from *C. reinhardtii*.

HCO_3^- AND CO_2 TRANSPORTERS—THE ESSENTIAL WORKERS OF CCMS

While much focus has been directed on the CO_2 concentrating organelles themselves, both carboxysome-based CCMs and pyrenoid-based CCMs need specialized carbonate and bicarbonate transporters for the elevation of the intracellular C_i concentration prior to CO_2 fixation (Findinier & Grossman, 2023; Price et al., 2011; Rottet et al., 2024). The structural and functional diversity among these transporters reflects adaptations to different cellular architectures and environmental niches, but all converge on the same core principles: active accumulation of HCO_3^-, strategic placement relative to the CO_2-fixing microcompartment, and carbonate transport regulation mechanisms to optimize photosynthetic efficiency.

In cyanobacteria, carboxysome-dependent CCMs rely on a suite of C_i uptake systems localized to the plasma membrane and sometimes the thylakoid membranes. The major transporters include BicA (the low-affinity, high-flux sodium-dependent bicarbonate transporter), the high-affinity SbtA (sodium-dependent), and CmpABCD (an ATP-binding cassette transporter for bicarbonate) (Figure 3a) (Omata et al., 1999; Price et al., 2004; Price & Howitt, 2014). SbtA from *Synechocystis* functions as a trimeric elevator-type transporter, shuttling HCO_3^- and Na^+ across the membrane via coordinated substrate-binding and large conformational changes. SbtA forms a stable complex with SbtB, which regulates SbtA's activity allosterically through AMP or cAMP binding (Fang et al., 2021; Selim et al., 2018; Shibata et al., 2002). The T-loop of SbtB locks SbtA in the inward-facing conformation (Liu et al., 2021). BicA, on the other hand, operates as a dimer with a C-terminal STAS domain required for activity and interacts with unknown regulatory proteins. These interactions may enable dynamic responses to changes in external and internal C_i concentration (Chan et al., 2022; Kurkela, 2020; Wang et al., 2019). The CmpABCD transporter in cyanobacteria consists of four subunits with distinct domains: CmpA is a periplasmic substrate-binding lipoprotein that uses a unique pocket and a coordinating calcium ion for specific high-affinity bicarbonate binding. CmpB forms the membrane channel, while CmpC and CmpD are ATP-binding domains that power the transport (Badger & Price, 2003). This configuration allows selective, high-affinity transport of HCO_3^-, tightly modulated by substrate availability and cytoplasmic ion balance (Koropatkin et al., 2007; Price et al., 2011).

In contrast to HCO_3^- transport, uptake of CO_2 does not play a major role for the cyanobacterial CCM. While CO_2 is imported under very low external CO_2 conditions, through CO_2 uptake systems (NDH-13/NDH-14 complexes), it is not a principal driver of the CCM (Price et al., 2013).

In eukaryotic algae, pyrenoid-based CCMs have evolved with a distinctly different set of transporters in accordance with subcellular compartmentalization. In *C. reinhardtii* and many diatoms, CO_2 and bicarbonate transport is coordinated across the plasma membrane, chloroplast envelope, and thylakoid membranes (Figure 3b). The key plasma membrane CO_2 channel (LCI1) provides passive CO_2 influx, while active HCO_3^- pumps first transport bicarbonate into the cytosol (HLA3 in *Chlamydomonas*, SLC4 in diatoms), and then into the stroma (LCIA in *Chlamydomonas*, unidentified in diatoms) (Kono et al., 2020; Nakajima et al., 2013; Yamano et al., 2015). Once inside the stroma, bestrophin-like channels (BST1-3) facilitate HCO_3^- movement into the thylakoid lumen, where the luminal CA CAH3 rapidly converts it to CO_2 (Mukherjee et al., 2019). Thylakoid tubules traverse the pyrenoid matrix, acting as a pipeline for newly generated CO_2 to reach Rubisco (Meyer et al., 2017).

Structurally, LCI1 and LCIA are integral membrane proteins with channel-like topology, mediating passive CO_2 flux under concentration gradients, but actively regulated by cellular C_i concentrations and environmental signals (Wang & Spalding, 2014). HLA3 and related pumps are members of the ABC (as Cmp in cyanobacteria) or SLC transporter families. Their ATPase domains couple ATP hydrolysis to substrate translocation and are vital for CCM function at low CO_2 concentrations (Duanmu et al., 2009; Prieß et al., 2018). BST channels are structurally related to bestrophin Ca^{2+} channels, with pore architectures adapted for HCO_3^- selectivity, and may form multimeric complexes to optimize ion flux (Bharill et al., 2014; Mackinder et al., 2017; Qu & Hartzell, 2008).

© 2026 The Author(s).

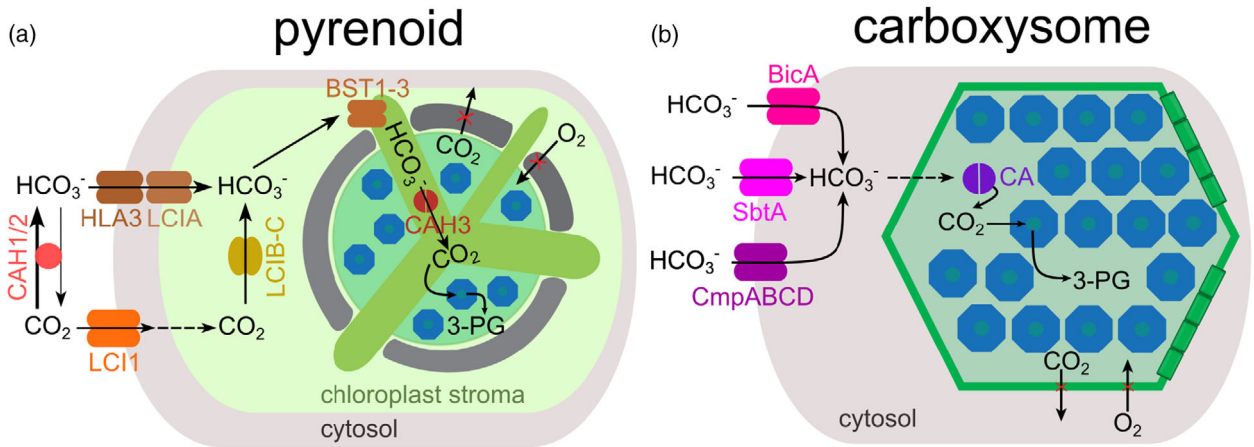


Figure 3. Different carbonate transporters in pyrenoids and carboxysomes.
(a) In pyrenoids, HLA3 and LCIA actively pump HCO_3^- across the plasma membrane, which is the main route for carbon uptake. The lesser-used LCI1 channels provide passive CO_2 influx, which is then converted into HCO_3^- by LCIB and LCIC. The HCO_3^- is then transported across the thylakoid membrane via the channels BST1-3 and then rapidly converted to CO_2 by the carbonic anhydrase (CA) CAH3.
(b) In carboxysomes, HCO_3^- is transported across the plasma membrane by the two sodium-dependent transporters BicA and SbtA and the ATP-binding cassette transporter CmpABCD. HCO_3^- then enters the carboxysomes via pores and is converted by the CA CsoSCA (α-carboxysomes) or γ-CA domain/β-CA CcaA (β-carboxysomes).

While both carboxysome-based and pyrenoid-based CCMs use an array of carbonate and bicarbonate transporters, carboxysome systems rely on bacterial-type transporters and direct cytosolic accumulation, whereas the eukaryotic pyrenoid systems utilize a more diverse set of transporters that are distributed across multiple membranes and employ specialized thylakoids that funnel CO_2 to Rubisco. Both systems rely on regulated permeability, spatial compartmentalization of CA activity, and dynamic transporter control in response to photosynthetic demand. Current and future engineering efforts to transplant CCMs into crops or industrial microorganisms are focusing on grafting these transporter modules alongside the microcompartment to reconstruct the full CCM for enhanced productivity.

DISCUSSION—COMPARING DIFFERENT BIOLOGICAL SOLUTIONS TO THE CO_2 CONCENTRATION LIMITATION

The striking structural divergence between carboxysomes and pyrenoids reflects convergent evolution under distinct evolutionary and ecological pressures. Both systems enable CO_2 fixation in low-CO_2 aquatic habitats, yet arose independently (He et al., 2023; Long et al., 2024; Rae et al., 2013). It is speculated that the first oxygenic photosynthesis machinery in cyanobacteria or their ancestors may have emerged around ~2300 mya (Raven et al., 2017). However, the first functional carboxysomes are hypothesized to have evolved ~350 mya in prokaryotic cyanobacteria, along with the appearance of pyrenoids in algae, while the first pyrenoids in hornworts are thought to have evolved ~100 mya ago (Badger & Price, 2003; Long et al., 2024; Rae et al., 2013; Villarreal & Renner, 2012). Recent phylogenetic, structural, and proteomic studies suggest that both pyrenoids and the two major carboxysome types have evolved convergently and likely originated multiple times in different lineages (Long et al., 2024; Moromizato et al., 2024; Rae et al., 2013).

A central factor for driving this diversity appears to be the environmental niche of these organisms. Except for a single lineage of land plants (hornworts), carboxysome or pyrenoid-containing organisms are aquatic photosynthetic organisms, meaning they are affected by the specific properties of CO_2 in water. In aquatic environments, CO_2 has a relatively low solubility and at typical seawater pH most dissolved inorganic carbon is present as HCO_3^- rather than free CO_2. Additionally, nutrient concentrations can fluctuate dramatically due to temperature, pH, and photosynthetic activity (Griffiths et al., 2017; Maberly & Gontero, 2017). Here, compartmentalizing the CO_2-fixation process inside protein microcompartments or LLPS organelles can elevate local CO_2 concentrations around Rubisco. These solutions seem tailored to water's diffusional limits, buffering external fluctuations, and minimizing photorespiratory waste (Griffiths et al., 2017; Long et al., 2021; Maberly & Gontero, 2017; Sarkar et al., 2024).

In terrestrial habitats, vascular plants face fundamentally different constraints. Atmospheric gas exchange is rapid, and diffusion is orders of magnitude faster than in water (Boston et al., 1989; Osmond et al., 1981). These observations could explain why vascular plants evolved biochemical CCMs, such as the C4 and the CAM pathway, which differ substantially from biophysical solutions. The biochemical strategies spatially (C4) or temporally (CAM) segregate initial CO_2 capture from Rubisco by exploiting

© 2026 The Author(s).

energetically expensive reactions to create local maxima in CO_2 concentration in specialized tissues or cellular compartments, notably bundle sheath cells in C4 plants (Dodd et al., 2002; Lopes et al., 2011). Currently, there is evidence for combining biophysical and biochemical CCMs for only a few algae species (i.e., *Ulva prolifera*) and the fresh water plant *Ottelia alismoides*, indicating that the two CCMs can be coordinated in a complementary manner depending on changing environmental conditions (Jiang et al., 2026; Zhang et al., 2025). Nonetheless, this appears to be a rare feature, and biophysical CCMs are thought to be the dominant pathway in marine algae (Matsuda et al., 2017). Similarly, there are aquatic and semi-aquatic embryophytes, such as *Hydrilla verticillata* and *Pilularia americana* that employ both C3 and C4 fixation pathways (Keeley, 1999; Reiskind et al., 1997; Xu et al., 2012). In general, however, rather than focusing on microcompartmental partitioning, terrestrial land plants exploit the capacity for active transport, membrane barriers, and cellular specialization driven by tissue differentiation (i.e., bundle sheath cells). These approaches are assumed to be more adapted to arid land environments where water loss and desiccation risk are dominant and where leaf and plant structures must maximize net carbon gain while minimizing photorespiration and water loss (Bräutigam et al., 2017; Osborne & Sack, 2012; Zhou et al., 2018).

Evolutionary lineage constraints may also play a role because microbial CCMs are assumed to have evolved a long time after the first endosymbiotic event and after the evolution of the first land plants (with the exception of *Paulinella*) (Gabr et al., 2020; Griffiths et al., 2017). While Raven et al. (2017) propose that *Gloeobacter*, the basal extant cyanobacterium, may have had CCMs already at the time of the Great Oxygenation Event (2300 mya), based on phylogenomic studies incorporating both protein and nucleotide data, as well as relaxed Bayesian molecular clock approaches (Blank & Sánchez-Baracaldo, 2010; Dillon & Castenholz, 1999; Olsson-Francis et al., 2010; Sánchez-Baracaldo, 2015; Sánchez-Baracaldo et al., 2014; Schirrmeister et al., 2015, 2016), other research shows that cyanobacteria evolved after the cyanobacteria crown group at around 350 mya, with no basal or stem group cyanobacteria extant (Butterfield, 2015; Lyons et al., 2014). Eukaryotic biophysical CCMs on the other hand, are consensually considered to have first appeared across algal lineages approximately 350 mya and in hornworts around 100 mya (Badger & Price, 2003; Meyer et al., 2017; Villarreal & Renner, 2012). These estimates correspond to a period during which various photosynthetic plant lineages had already been established and, hence, far after endosymbiosis. Additionally, the evolutionary data indicates that pyrenoids evolved multiple times independently via convergent evolution and, in the case of hornworts, they were lost and regained at least five times (Meyer, Goudet, & Griffiths, 2020; Rae et al., 2013; Raven et al., 2017; Villarreal & Renner, 2012). In comparison, complex multicellular land plants are limited in their evolutionary potential by slower rates of organelle innovation, developmental constraints, and the high energetic burden of maintaining microcompartments at cellular scales appropriate for larger organisms. These considerations may also explain the absence of microbial-like CCMs in almost all terrestrial plants (He et al., 2023; Rae et al., 2013; Villarreal & Renner, 2012).

Overall, we still lack an in depth and mechanistic understanding for the plethora of approaches to concentrate CO_2. To overcome this lack of knowledge and to enhance the photosynthetic efficiency of land plants, there has been extensive research in the past years to integrate microbial CCMs into crop species for improved growth rate and yield. Morphologically correct α-carboxysomes containing cyanobacterial Rubisco, as well as key linker and shell proteins, have been shown to support autotrophic growth and enhanced photosynthesis in tobacco at elevated CO_2. Although the transgenic plants were unable to grow under ambient air, the study provides a proof-of-concept that functional CCMs can operate within a C3 chloroplast background (Chen et al., 2023). In addition to transplanting native cyanobacterial components of the CCM into plants, future studies could also implement directed evolution approaches and novel synthetic systems to create a plant-based CCM (Nguyen et al., 2024). Complementary work on pyrenoid-based CCMs investigates the minimal modules needed to increase the concentration of CO_2 near Rubisco, emphasizing microcompartments and CA relocalization as the next milestones toward fully functional microbial CCMs in major crop species (Adler et al., 2022).

OUTLOOK

Despite major progress enabled by high-resolution structural biology, advanced microscopy, and modern molecular biology, crucial aspects of microbial CCMs remain only partially understood. Recent studies have resolved the atomic architecture of carboxysome and pyrenoid shells, mapped the spatial organization of Rubisco and CA, and reconstructed partially functional CCM modules in non-native organisms. However, the mechanism of selective permeability remains opaque: it is not clear how carboxysome shell pores distinguish between anionic bicarbonate, uncharged CO_2, O_2, and at the same time larger metabolites such as RuBP. Quantifying the dynamic selectivity, gating behavior, and modulation of specific shell protein variants is necessary to fully understand carboxysome function and regulation.

Beyond selectivity, the evolutionary drivers underlying the diversity of CCMs pose deep biological questions. Why has nature repeatedly solved the Rubisco problem with such a variety of approaches? Environmental constraints,

© 2026 The Author(s).

Box 1. Key remaining questions

- How is the dynamic selectivity of biophysical CCMs mechanistically enforced?
- What are the mechanistic factors for the evolution of specific CCM architectures?
- How are the protein stoichiometry, CCM assembly, and regulation in native organisms controlled and how can this be applied to eventual transplantation into plants?

lineage-specific genetic toolkits, and physical limitations seem to force the trajectories, but the exact causal factors and why higher plants never adopted microbial solutions or lack a CCM, such as C3 plants, remain unanswered.

A challenge for translation is engineering CCMs into non-native, high-yield phototrophic systems for agriculture and biotechnology. Recent synthetic biology approaches demonstrate architectural feasibility. However, attempts at creating functional heterologous reconstitutions in plants showing enhanced photosynthesis have mostly failed. In one case, reconstitution in tobacco succeeded but led to reduced growth in ambient air. This shows that building functional carboxysomes or pyrenoid-like organelles in plants or microbes requires precise control over enzyme stoichiometry, shell assembly, metabolite transport, and cofactor regulation, highlighting our limited understanding of biophysical CCMs and, hence, poses major difficulties for applications. In conclusion, not only are further efforts into understanding the fundamental biochemistry and biophysics of CCMs needed, but also more work on the bottom-up engineering of CCMs is required (Box 1).

ACKNOWLEDGEMENTS

C. E. M. F. and A. M. K. are grateful for the generous support from the Max Planck Foundation and Max Planck Society. Open Access funding enabled and organized by Projekt DEAL.

CONFLICT OF INTEREST

None of the authors have a conflict of interest to disclose.

DATA AVAILABILITY STATEMENT

Data sharing not applicable to this article as no datasets were generated or analysed during the current study.

REFERENCES

Abernathy, M.H., **Czajka, J.J.**, **Allen, D.K.**, **Hill, N.C.**, **Cameron, J.C.** & **Tang, Y.J.** (2019) Cyanobacterial carboxysome mutant analysis reveals the influence of enzyme compartmentalization on cellular metabolism and metabolic network rigidity. *Metabolic Engineering*, **54**, 222–231.

Adler, L., **Díaz-Ramos, A.**, **Mao, Y.**, **Pukacz, K.R.**, **Fei, C.** & **McCormick, A.J.** (2022) New horizons for building pyrenoid-based CO_2-concentrating mechanisms in plants to improve yields. *Plant Physiology*, **190**, 1609–1627.

Adler, L., **Lau, C.S.**, **Shaikh, K.M.**, **van Maldegem, K.A.**, **Payne-Dwyer, A.L.**, **Lefoulon, C.** ***et al.*** (2023) The role of BST4 in the pyrenoid of *Chlamydomonas reinhardtii*. *bioRxiv*. Available from: https://doi.org/10.1101/2023.06.15.545204

Atkinson, N., **Feike, D.**, **Mackinder, L.C.M.**, **Meyer, M.T.**, **Griffiths, H.**, **Jonikas, M.C.** ***et al.*** (2016) Introducing an algal carbon-concentrating mechanism into higher plants: location and incorporation of key components. *Plant Biotechnology Journal*, **14**, 1302–1315.

Atkinson, N., **Mao, Y.**, **Chan, K.X.** & **McCormick, A.J.** (2020) Condensation of rubisco into a proto-pyrenoid in higher plant chloroplasts. *Nature Communications*, **11**, 6303.

Atkinson, N., **Stringer, R.**, **Mitchell, S.R.**, **Seung, D.** & **McCormick, A.J.** (2024) SAGA1 and SAGA2 promote starch formation around proto-pyrenoids in Arabidopsis chloroplasts. *Proceedings of the National Academy of Sciences of the United States of America*, **121**, e2311013121.

Badger, M.R. & **Price, G.D.** (2003) CO_2 concentrating mechanisms in cyanobacteria: molecular components, their diversity and evolution. *Journal of Experimental Botany*, **54**, 609–622.

Barrett, J., **Girr, P.** & **Mackinder, L.C.M.** (2021) Pyrenoids: CO_2-fixing phase separated liquid organelles. *Biochimica et Biophysica Acta (BBA) - Molecular Cell Research*, **1868**, 118949.

Barrett, J., **Naduthodi, M.I.S.**, **Mao, Y.**, **Dégut, C.**, **Musiał, S.**, **Salter, A.** ***et al.*** (2024) A promiscuous mechanism to phase separate eukaryotic carbon fixation in the green lineage. *Nature Plants*, **10**, 1801–1813.

Bharill, S., **Fu, Z.**, **Palty, R.** & **Isacoff, E.Y.** (2014) Stoichiometry and specific assembly of best ion channels. *Proceedings of the National Academy of Sciences of the United States of America*, **111**, 6491–6496.

Blank, C.E. & **Sánchez-Baracaldo, P.** (2010) Timing of morphological and ecological innovations in the cyanobacteria - a key to understanding the rise in atmospheric oxygen. *Geobiology*, **8**, 1–23.

Blikstad, C., **Dugan, E.J.**, **Laughlin, T.G.**, **Turnšek, J.B.**, **Liu, M.D.**, **Shoemaker, S.R.** ***et al.*** (2023) Identification of a carbonic anhydrase–rubisco complex within the alpha-carboxysome. *Proceedings of the National Academy of Sciences of the United States of America*, **120**, e2308600120.

Boston, H.L., **Adams, M.S.** & **Madsen, J.D.** (1989) Photosynthetic strategies and productivity in aquatic systems. *Aquatic Botany*, **34**, 27–57.

Bräutigam, A., **Schlüter, U.**, **Eisenhut, M.** & **Gowik, U.** (2017) On the evolutionary origin of CAM photosynthesis. *Plant Physiology*, **174**, 473–477.

Butterfield, N.J. (2015) Proterozoic photosynthesis - a critical review. *Palaeontology*, **58**, 953–972.

Cai, F., **Dou, Z.**, **Bernstein, S.L.**, **Leverenz, R.**, **Williams, E.B.**, **Heinhorst, S.** ***et al.*** (2015) Advances in understanding carboxysome assembly in *Prochlorococcus* and *Synechococcus* implicate CsoS2 as a critical component. *Life*, **5**, 1141–1171.

Cameron, J.C., **Wilson, S.C.**, **Bernstein, S.L.** & **Kerfeld, C.A.** (2013) Biogenesis of a bacterial organelle: the carboxysome assembly pathway. *Cell*, **155**, 1131–1140.

Catherall, E., **Musial, S.**, **Atkinson, N.**, **Walker, C.E.**, **Mackinder, L.C.M.** & **McCormick, A.J.** (2025) From algae to plants: understanding pyrenoid-based CO_2-concentrating mechanisms. *Trends in Biochemical Sciences*, **50**, 33–45.

Chan, M., **Alfawaz, Y.**, **Paul, A.** & **Shukla, D.** (2022) Elevator-type mechanism of the cyanobacterial bicarbonate transporter. *bioRxiv*. Available from: https://doi.org/10.1101/2022.06.08.495363

Chen, T., **Hojka, M.**, **Davey, P.**, **Sun, Y.**, **Dykes, G.F.**, **Zhou, F.** ***et al.*** (2023) Engineering α-carboxysomes into plant chloroplasts to support autotrophic photosynthesis. *Nature Communications*, **14**, 2118.

Dao, O., **Bertrand, M.**, **Alseekh, S.**, **Veillet, F.**, **Auroy, P.**, **Nguyen, P.C.** ***et al.*** (2025) The green algae CO_2 concentrating mechanism and photorespiration jointly operate during acclimation to low CO_2. *Nature Communications*, **16**, 5296.

de Pins, B., **Malbranke, C.**, **Jabłońska, J.**, **Shmuel, A.**, **Sharon, I.**, **Bitbol, A.F.** ***et al.*** (2025) Rubisco is slow across the tree of life. *Proceedings of the National Academy of Sciences of the United States of America*, **122**(47), e2501433122.

Dillon, J.G. & **Castenholz, R.W.** (1999) Scytonemin, a cyanobacterial sheath pigment, protects against UVC radiation: implications for early photosynthetic life. *Journal of Phycology*, **35**, 673–681.

Dodd, A.N., **Borland, A.M.**, **Haslam, R.P.**, **Griffiths, H.** & **Maxwell, K.** (2002) Crassulacean acid metabolism: plastic, fantastic. *Journal of Experimental Botany*, **53**, 569–580.

© 2026 The Author(s).

Duanmu, D., **Miller, A.R.**, **Horken, K.M.**, **Weeks, D.P.** & **Spalding, M.H.** (2009) Knockdown of limiting-CO_2-induced gene HLA3 decreases HCO_3^- transport and photosynthetic Ci affinity in *Chlamydomonas reinhardtii*. *PNAS*, **106**, 5990–5995.

Engel, B.D., **Schaffer, M.**, **Cuellar, L.K.**, **Villa, E.**, **Plitzko, J.M.** & **Baumeister, W.** (2015) Native architecture of the *Chlamydomonas* chloroplast revealed by in situ cryo-electron tomography. *eLife*, **4**, e04889.

Evans, S.L., **Al-Hazeem, M.M.J.**, **Mann, D.**, **Smetacek, N.**, **Beavil, A.J.**, **Sun, Y.** ***et al.*** (2023) Single-particle cryo-EM analysis of the shell architecture and internal organization of an intact α-carboxysome. *Structure*, **31**, 677–688.

Fang, S., **Huang, X.**, **Zhang, X.**, **Zhang, M.**, **Hao, Y.**, **Guo, H.** ***et al.*** (2021) Molecular mechanism underlying transport and allosteric inhibition of bicarbonate transporter SbtA. *PNAS*, **118**, e2101632118.

Faulkner, M., **Rodriguez-Ramos, J.**, **Dykes, G.F.**, **Owen, S.V.**, **Casella, S.**, **Simpson, D.M.** ***et al.*** (2017) Direct characterization of the native structure and mechanics of cyanobacterial carboxysomes. *Nanoscale*, **9**, 10662–10673.

Faulkner, M., **Szabó, I.**, **Weetman, S.L.**, **Sicard, F.**, **Huber, R.G.**, **Bond, P.J.** ***et al.*** (2020) Molecular simulations unravel the molecular principles that mediate selective permeability of carboxysome shell protein. *Scientific Reports*, **10**, 17501.

Fei, C., **Wilson, A.T.**, **Mangan, N.M.**, **Wingreen, N.S.** & **Jonikas, M.C.** (2022) Modelling the pyrenoid-based CO_2-concentrating mechanism provides insights into its operating principles and a roadmap for its engineering into crops. *Nature Plants*, **8**, 583–595.

Fei, C., **Wingreen, N.S.** & **Jonikas, M.C.** (2025) A pyrenoid-based CO_2-concentrating mechanism can be effective and efficient even under scenarios of high membrane CO_2 permeability. *Plant Physiology*, **198**, kiaf316.

Findinier, J. & **Grossman, A.R.** (2023) One step further toward a crop CO_2-concentrating mechanism. *Journal of Experimental Botany*, **74**, 3402–3405.

Flamholz, A. & **Shih, P.M.** (2020) Cell biology of photosynthesis over geologic time. *Current Biology*, **30**, 490–494.

Flamholz, A.I., **Dugan, E.**, **Blikstad, C.**, **Gleizer, S.**, **Ben-Nissan, R.**, **Amram, S.** ***et al.*** (2020) Functional reconstitution of a bacterial CO_2 concentrating mechanism in *Escherichia coli*. *eLife*, **9**, 1–57.

Flamholz, A.I., **Dugan, E.**, **Panich, J.**, **Desmarais, J.J.**, **Oltrogge, L.M.**, **Fischer, W.W.** ***et al.*** (2022) Trajectories for the evolution of bacterial CO_2-concentrating mechanisms. *Proceedings of the National Academy of Sciences of the United States of America*, **119**, e2210539119.

Franklin, E., **Wang, L.**, **Cruz, E.R.**, **Duggal, K.**, **Ergun, S.L.**, **Garde, A.** ***et al.*** (2026) Proteomic analysis of the pyrenoid-traversing membranes of *Chlamydomonas reinhardtii* reveals novel components. *New Phytologist*, **249**, 359–372.

Freeman Rosenzweig, E.S., **Xu, B.**, **Kuhn Cuellar, L.**, **Martinez-Sanchez, A.**, **Schaffer, M.**, **Strauss, M.** ***et al.*** (2017) The eukaryotic CO_2-concentrating organelle is liquid-like and exhibits dynamic reorganization. *Cell*, **171**, 148–162.

Fuchs, G. (2011) Alternative pathways of carbon dioxide fixation: insights into the early evolution of life? *Annual Review of Microbiology*, **65**, 631–658.

Gabr, A., **Grossman, A.R.** & **Bhattacharya, D.** (2020) *Paulinella*, a model for understanding plastid primary endosymbiosis. *Journal of Phycology*, **56**, 837–843.

Gantt, E. & **Conti, S.F.** (1969) Ultrastructure of blue-green algae. *Journal of Bacteriology*, **97**, 1486–1493.

Griffiths, D.J. (1970) The pyrenoid. *The Botanical Review*, **36**, 29–58.

Griffiths, H., **Meyer, M.T.** & **Rickaby, R.E.M.** (2017) Overcoming adversity through diversity: aquatic carbon concentrating mechanisms. *Journal of Experimental Botany*, **68**, 3689–3695.

Hanson, M.R., **Lin, M.T.**, **Carmo-Silva, A.E.** & **Parry, M.A.J.** (2016) Towards engineering carboxysomes into C3 plants. *The Plant Journal*, **87**, 38–50.

Hatch, M.D. & **Slack, C.R.** (1966) Photosynthesis by sugar-cane leaves: a new carboxylation reaction and the pathway of sugar formation. *The Biochemical Journal*, **101**, 103–111.

He, S., **Chou, H.T.**, **Matthies, D.**, **Wunder, T.**, **Meyer, M.T.**, **Atkinson, N.** ***et al.*** (2020) The structural basis of rubisco phase separation in the pyrenoid. *Nature Plants*, **6**, 1480–1490.

He, S., **Crans, V.L.** & **Jonikas, M.C.** (2023) The pyrenoid: the eukaryotic CO_2-concentrating organelle. *Plant Cell*, **35**, 3236–3259.

Hennacy, J.H., **Atkinson, N.**, **Kayser-Browne, A.**, **Ergun, S.L.**, **Franklin, E.**, **Wang, L.** ***et al.*** (2024) SAGA1 and MITH1 produce matrix-traversing-membranes in the CO_2-fixing pyrenoid. *Nature Plants*, **10**, 2038–2051.

Hennacy, J.H. & **Jonikas, M.C.** (2020) Prospects for engineering biophysical CO_2 concentrating mechanisms into land plants to enhance yields. *Annual Review of Plant Biology*, **71**, 461–485.

Hill, N.C., **Tay, J.W.**, **Altus, S.**, **Bortz, D.M.** & **Cameron, J.C.** (2020) Life cycle of a cyanobacterial carboxysome. *Science Advances*, **6**, eaba1269.

Huang, F., **Kong, W.-W.**, **Sun, Y.**, **Chen, T.**, **Dykes, G.F.**, **Jiang, Y.-L.** ***et al.*** (2020) Rubisco accumulation factor 1 (Raf1) plays essential roles in mediating rubisco assembly and carboxysome biogenesis. *PNAS*, **117**, 17418–17428.

Huang, J., **Jiang, Q.**, **Yang, M.**, **Dykes, G.F.**, **Weetman, S.L.**, **Xin, W.** ***et al.*** (2022) Probing the internal pH and permeability of a carboxysome shell. *Biomacromolecules*, **23**, 4339–4348.

Huffine, C.A., **Fontana, C.**, **Avramov, A.**, **Sempeck, C.** & **Cameron, J.C.** (2024) *Cyanobacteria form a procarboxysome-like structure in response to high CO_2*. Available from: https://doi.org/10.1101/2024.06.28.601118

Huffine, C.A., **Zhao, R.**, **Tang, Y.J.** & **Cameron, J.C.** (2023) Role of carboxysomes in cyanobacterial CO_2 assimilation: CO_2 concentrating mechanisms and metabolon implications. *Environmental Microbiology*, **25**, 219–228.

Iglesias, A., **Gonzalez, D.** & **Andreo, C.** (1987) Crassulacean acid metabolism: a pathway for photosynthetic CO_2 fixation in arid habitats. *Biochemical Education*, **15**, 111–115.

Itakura, A.K., **Chan, K.X.**, **Atkinson, N.**, **Pallesen, L.**, **Wang, L.**, **Reeves, G.** ***et al.*** (2019) A rubisco-binding protein is required for normal pyrenoid number and starch sheath morphology in *Chlamydomonas reinhardtii*. *Proceedings of the National Academy of Sciences of the United States of America*, **116**, 18445–18454.

Jiang, H.S., **Huang, W.**, **Han, S.**, **Li, P.**, **Liao, Z.**, **Wei, L.** ***et al.*** (2026) A novel single-cell NAD-ME C4 subtype integrated with CAM and bicarbonate use in an aquatic plant. *New Phytologist*, **249**, 2386–2401.

Kaplan, A. & **Reinhold, L.** (1999) CO_2 concentrating mechanisms in photosynthetic microorganisms. *Annual Review of Plant Physiology and Plant Molecular Biology*, **50**, 539–570.

Keeley, J.E. (1999) Photosynthetic pathway diversity in a seasonal pool community. *Functional Ecology*, **13**, 106–118.

Kerfeld, C.A., **Sawaya, M.R.**, **Tanaka, S.**, **Nguyen, C.V.**, **Phillips, M.**, **Beeby, M.** ***et al.*** (2005) Protein structures forming the shell of primitive bacterial organelles. *Science*, **309**, 936–938.

Kinney, J.N., **Salmeen, A.**, **Cai, F.** & **Kerfeld, C.A.** (2012) Elucidating essential role of conserved carboxysomal protein CcmN reveals common feature of bacterial microcompartment assembly. *Journal of Biological Chemistry*, **287**, 17729–17736.

Kong, W.W., **Zhu, Y.**, **Zhao, H.R.**, **du, K.**, **Zhou, R.Q.**, **Li, B.** ***et al.*** (2024) Cryo-electron tomography reveals the packaging pattern of RuBisCOs in *Synechococcus* β-carboxysome. *Structure*, **32**, 1110–1120.

Kono, A., **Chou, T.H.**, **Radhakrishnan, A.**, **Bolla, J.R.**, **Sankar, K.**, **Shome, S.** ***et al.*** (2020) Structure and function of LCI1: a plasma membrane CO_2 channel in the *Chlamydomonas* CO_2 concentrating mechanism. *Plant Journal*, **102**, 1107–1126.

Koropatkin, N.M., **Koppenaal, D.W.**, **Pakrasi, H.B.** & **Smith, T.J.** (2007) The structure of a cyanobacterial bicarbonate transport protein, CmpA. *Journal of Biological Chemistry*, **282**, 2606–2614.

Kortschak, H.P., **Hartt, C.E.** & **Burr, G.** (1965) Carbon dioxide fixation in sugarcane leaves. *Plant Physiology*, **40**, 209–213.

Kroth, P.G. (2015) The biodiversity of carbon assimilation. *Journal of Plant Physiology*, **172**, 76–81.

Küffner, A.M., **Pommerenke, B.**, **Kley, L.**, **Ng, J.Z.Y.**, **Prinz, S.**, **Tinzl-Zechner, M.** ***et al.*** (2024) *Bottom-up reconstruction of minimal pyrenoids provides insights into the evolution and mechanisms of carbon concentration by EPYC1 proteins*. Available from: https://doi.org/10.1101/2024.06.28.601168

Kurkela, J. (2020) The biological role of omega subunit of cyanobacterial RNA polymerase. [Diss. PhD thesis]. In: *Annales Universitatis Turkuensis, Ser AI: 630*. Turku: University of Turku.

Kusel-Fetzmann, E. & **Weidinger, M.** (2008) Ultrastructure of five euglena species positioned in the subdivision Serpentes. *Protoplasma*, **233**, 209–222.

© 2026 The Author(s).

Lacoste-Royal, G. & **Gibbs, S.P.** (1987) Immunocytochemical localization of ribulose-1,5-bisphosphate carboxylase in the pyrenoid and thylakoid region of the chloroplast of *Chlamydomonas reinhardtii*. *Plant Physiology*, **83**, 602–606.

Li, T., **Chen, T.**, **Chang, P.**, **Ge, X.**, **Chriscoli, V.**, **Dykes, G.F.** ***et al.*** (2024) Uncovering the roles of the scaffolding protein CsoS2 in mediating the assembly and shape of the α-carboxysome shell. *MBio*, **15**, e01358-24.

Li, T., **Jiang, Q.**, **Huang, J.**, **Aitchison, C.M.**, **Huang, F.**, **Yang, M.** ***et al.*** (2020) Reprogramming bacterial protein organelles as a nanoreactor for hydrogen production. *Nature Communications*, **11**(1), 5448.

Li, Y., **Kennedy, N.W.**, **Li, S.**, **Mills, C.E.**, **Tullman-Ercek, D.** & **Olvera De La Cruz, M.** (2021) Computational and experimental approaches to controlling bacterial microcompartment assembly. *ACS Central Science*, **7**, 658–670.

Liang, B., **Zhao, Y.** & **Yang, J.** (2020) Recent advances in developing artificial autotrophic microorganism for reinforcing CO_2 fixation. *Frontiers in Microbiology*, **11**, 592631.

Lin, M.T., **Occhialini, A.**, **Andralojc, P.J.**, **Devonshire, J.**, **Hines, K.M.**, **Parry, M.A.J.** ***et al.*** (2014) β-Carboxysomal proteins assemble into highly organized structures in *Nicotiana* chloroplasts. *Plant Journal*, **79**, 1–12.

Liu, X.Y., **Hou, W.T.**, **Wang, L.**, **Li, B.**, **Chen, Y.**, **Chen, Y.** ***et al.*** (2021) Structures of cyanobacterial bicarbonate transporter SbtA and its complex with PII-like SbtB. *Cell Discovery*, **7**, 63.

Long, B.M., **Förster, B.**, **Pulsford, S.B.**, **Dean Price, G.** & **Badger, M.R.** (2021) Rubisco proton production can drive the elevation of CO_2 within condensates and carboxysomes. *PNAS*, **118**, e2014406118.

Long, B.M., **Hee, W.Y.**, **Sharwood, R.E.**, **Rae, B.D.**, **Kaines, S.**, **Lim, Y.L.** ***et al.*** (2018) Carboxysome encapsulation of the CO_2-fixing enzyme rubisco in tobacco chloroplasts. *Nature Communications*, **9**, 3570.

Long, B.M., **Matsuda, Y.** & **Moroney, J.V.** (2024) Algal chloroplast pyrenoids: evidence for convergent evolution. *Proceedings of the National Academy of Sciences of the United States of America*, **121**, e2402546121.

Lopes, M.S., **Araus, J.L.**, **Van Heerden, P.D.R.** & **Foyer, C.H.** (2011) Enhancing drought tolerance in C4 crops. *Journal of Experimental Botany*, **62**, 3135–3153.

Lyons, T.W., **Reinhard, C.T.** & **Planavsky, N.J.** (2014) Evolution: a fixed-nitrogen fix in the early ocean? *Current Biology*, **24**, R276–R278.

Maberly, S.C. & **Gontero, B.** (2017) Ecological imperatives for aquatic CO_2-concentrating mechanisms. *Journal of Experimental Botany*, **68**, 3797–3814.

Mackinder, L.C.M., **Chen, C.**, **Leib, R.D.**, **Patena, W.**, **Blum, S.R.**, **Rodman, M.** ***et al.*** (2017) A spatial interactome reveals the protein organization of the algal CO_2-concentrating mechanism. *Cell*, **171**, 133–147.

Mackinder, L.C.M., **Meyer, M.T.**, **Mettler-Altmann, T.**, **Chen, V.K.**, **Mitchell, M.C.**, **Caspari, O.** ***et al.*** (2016) A repeat protein links rubisco to form the eukaryotic carbon-concentrating organelle. *Proceedings of the National Academy of Sciences of the United States of America*, **113**, 5958–5963.

Mahinthichaichan, P., **Morris, D.M.**, **Wang, Y.**, **Jensen, G.J.** & **Tajkhorshid, E.** (2018) Selective permeability of carboxysome shell pores to anionic molecules. *Journal of Physical Chemistry B*, **122**, 9110–9118.

Mangan, N. & **Brenner, M.** (2014) Systems analysis of the CO_2 concentrating mechanism in cyanobacteria. *eLife*, **3**, e02043.

Mangan, N.M., **Flamholz, A.**, **Hood, R.D.**, **Milo, R.** & **Savage, D.F.** (2016) pH determines the energetic efficiency of the cyanobacterial CO_2 concentrating mechanism. *Proceedings of the National Academy of Sciences of the United States of America*, **113**, E5354–E5362.

Matsuda, Y., **Hopkinson, B.M.**, **Nakajima, K.**, **Dupont, C.L.** & **Tsuji, Y.** (2017) Mechanisms of carbon dioxide acquisition and CO_2 sensing in marine diatoms: a gateway to carbon metabolism. *Philosophical Transactions of the Royal Society, B: Biological Sciences*, **372**, 20160403.

McKay, R.M.L. & **Gibbs, S.P.** (1990) Phycoerythrin is absent from the pyrenoid of *Porphyridium cruentum*: photosynthetic implications. *Planta*, **180**, 249–256.

Melnicki, M.R., **Sutter, M.** & **Kerfeld, C.A.** (2021) Evolutionary relationships among shell proteins of carboxysomes and metabolosomes. *Current Opinion in Microbiology*, **63**, 1–9.

Menon, B.B., **Dou, Z.**, **Heinhorst, S.**, **Shively, J.M.** & **Cannon, G.C.** (2008) *Halothiobacillus neapolitanus* Carboxysomes Sequester Heterologous and Chimeric RubisCO Species. *PLoS One*, **3**, e3570. Available from: https://doi.org/10.1371/journal.pone.0003570

Meyer, M. & **Griffiths, H.** (2013) Origins and diversity of eukaryotic CO_2-concentrating mechanisms: lessons for the future. *Journal of Experimental Botany*, **64**, 769–786.

Meyer, M.T., **Goudet, M.M.** & **Griffiths, H.** (2020) The algal pyrenoid. In: Larkum, A., Grossman, A. & Raven, J. (Eds.) *Photosynthesis in algae: biochemical and physiological mechanisms. Advances in photosynthesis and respiration*, Vol. **45**. Cham: Springer.

Meyer, M.T., **Itakura, A.K.**, **Patena, W.**, **Wang, L.**, **He, S.**, **Emrich-Mills, T.** ***et al.*** (2020) Assembly of the algal CO_2-fixing organelle, the pyrenoid, is guided by a rubisco-binding motif. *Science Advances*, **6**, eabd2408.

Meyer, M.T., **Whittaker, C.** & **Griffiths, H.** (2017) The algal pyrenoid: key unanswered questions. *Journal of Experimental Botany*, **68**, 3739–3749.

Moromizato, R., **Fukuda, K.**, **Suzuki, S.**, **Motomura, T.**, **Nagasato, C.** & **Hirakawa, Y.** (2024) Pyrenoid proteomics reveals independent evolution of the CO_2-concentrating organelle in chlorarachniophytes. *Proceedings of the National Academy of Sciences of the United States of America*, **121**, e3218542121.

Mueller-Cajar, O., **Stotz, M.**, **Wendler, P.**, **Hartl, F.U.**, **Bracher, A.** & **Hayer-Hartl, M.** (2011) Structure and function of the AAA+ protein CbbX, a red-type Rubisco activase. *Nature*, **479**, 194–199.

Mukherjee, A., **Lau, C.S.**, **Walker, C.E.**, **Rai, A.K.**, **Prejean, C.I.**, **Yates, G.** ***et al.*** (2019) Thylakoid localized bestrophin-like proteins are essential for the CO_2 concentrating mechanism of *Chlamydomonas reinhardtii*. *Proceedings of the National Academy of Sciences of the United States of America*, **116**, 16915–16920.

Nagasato, C. & **Motomura, T.** (2002) New pyrenoid formation in the brown alga, *Scytosiphon lomentaria* (Scytosiphonales, Phaeophyceae). *Journal of Phycology*, **38**, 800–806.

Nakajima, K., **Tanaka, A.** & **Matsuda, Y.** (2013) SLC4 family transporters in a marine diatom directly pump bicarbonate from seawater. *Proceedings of the National Academy of Sciences of the United States of America*, **110**, 1767–1772.

Nam, O., **Musiał, S.**, **Demulder, M.**, **McKenzie, C.**, **Dowle, A.**, **Dowson, M.** ***et al.*** (2024) A protein blueprint of the diatom CO_2-fixing organelle. *Cell*, **187**, 5935–5950.

Neofotis, P., **Temple, J.**, **Tessmer, O.L.**, **Bibik, J.**, **Norris, N.**, **Pollner, E.** ***et al.*** (2021) The induction of pyrenoid synthesis by hyperoxia and its implications for the natual diversity of photosynthetic responses in *Chlamydomonas*. *Elife*, **10**.

Nguyen, N.D., **Pulsford, S.B.**, **Förster, B.**, **Rottet, S.**, **Rourke, L.**, **Long, B.M.** ***et al.*** (2024) A carboxysome-based CO_2 concentrating mechanism for C3 crop chloroplasts: advances and the road ahead. *Plant Journal*, **118**, 940–952.

Ni, T., **Jiang, Q.**, **Ng, P.C.**, **Shen, J.**, **Dou, H.**, **Zhu, Y.** ***et al.*** (2023) Intrinsically disordered CsoS2 acts as a general molecular thread for α-carboxysome shell assembly. *Nature Communications*, **14**, 5512.

Ni, T., **Sun, Y.**, **Burn, W.**, **Al-Hazeem, M.M.J.**, **Zhu, Y.**, **Yu, X.** ***et al.*** (2022) Structure and assembly of cargo Rubisco in two native α-carboxysomes. *Nature Communications*, **13**, 4299.

Niederhuber, M.J., **Lambert, T.J.**, **Yapp, C.**, **Silver, P.A.** & **Polka, J.K.** (2017) Superresolution microscopy of the β-carboxysome reveals a homogeneous matrix. *Molecular Biology of the Cell*, **28**, 2734–2745.

Ochoa, J.M., **Mijares, O.**, **Acosta, A.A.**, **Escoto, X.**, **Leon-Rivera, N.**, **Marshall, J.D.** ***et al.*** (2021) Structural characterization of hexameric shell proteins from two types of choline-utilization bacterial microcompartments. *Acta crystallographica. Section F, Structural Biology Communications*, **77**, 275–285.

Oh, Z.G., **Ang, W.S.L.**, **Poh, C.W.**, **Lai, S.K.**, **Sze, S.K.**, **Li, H.Y.** ***et al.*** (2023) A linker protein from a red-type pyrenoid phase separates with rubisco via oligomerizing sticker motifs. *Proceedings of the National Academy of Sciences of the United States of America*, **120**, e2304833120.

Ohad, I., **Siekevitz, P.** & **Palade, G.E.** (1967) Biogenesis of chloroplast membranes I. Plastid dedifferentiation in a dark-grown algal mutant (*Chlamydomonas reinhardi*). *The Journal of Cell Biology*, **35**, 521–552.

Olsson-Francis, K., **De La Torre, R.** & **Cockell, C.S.** (2010) Isolation of novel extreme-tolerant cyanobacteria from a rock-dwelling microbial community by using exposure to low earth orbit. *Applied and Environmental Microbiology*, **76**, 2115–2121.

Oltrogge, L.M., **Chaijarasphong, T.**, **Chen, A.W.**, **Bolin, E.R.**, **Marqusee, S.** & **Savage, D.F.** (2020) Multivalent interactions between CsoS2 and rubisco

© 2026 The Author(s).

mediate α-carboxysome formation. *Nature Structural & Molecular Biology*, **27**, 281–287.

Oltrogge, L.M., **Chen, A.W.**, **Chaijarasphong, T.**, **Turnšek, J.B.** & **Savage, D.F.** (2024) α-Carboxysome size is controlled by the disordered scaffold protein CsoS2. *Biochemistry*, **63**, 219–229.

Omata, T., **Dean Price, G.**, **Badger, M.R.**, **Okamura, M.**, **Gohta, S.** & **Ogawa, T.** (1999) Identification of an ATP-binding cassette transporter involved in bicarbonate uptake in the cyanobacterium *Synechococcus* sp. strain PCC 7942. *PNAS*, **96**, 13571–13576.

Orr, D.J., **Worrall, D.**, **Lin, M.T.**, **Carmo-Silva, E.**, **Hanson, M.R.** & **Parry, M.A.J.** (2020) Hybrid cyanobacterial-tobacco rubisco supports autotrophic growth and procarboxysomal aggregation. *Plant Physiology*, **182**, 807–818.

Osborne, C.P. & **Sack, L.** (2012) Evolution of C4 plants: a new hypothesis for an interaction of CO_2 and water relations mediated by plant hydraulics. *Philosophical Transactions of the Royal Society, B: Biological Sciences*, **367**, 583–600.

Osmond, C.B., **Valaane, N.**, **Haslam, S.M.**, **Uotila, P.** & **Roksandic, Z.** (1981) Comparisons of delta13C values in leaves of aquatic macrophytes from different habitats in Britain and Finland; some implications for photosynthetic processes in aquatic plants. *Oecologia (Berl)*, **50**, 117–124.

Price, G.D. & **Badger, M.R.** (1989a) Expression of human carbonic anhydrase in the cyanobacterium *Synechococcus* PCC7942 creates a high CO_2-requiring phenotype, evidence for a central role for carboxysomes in the CO_2 concentrating mechanism. *Plant Physiology*, **91**, 505–513.

Price, G.D. & **Badger, M.R.** (1989b) Isolation and characterization of high CO_2-requiring-mutants of the cyanobacterium *Synechococcus* PCC7942: two phenotypes that accumulate inorganic carbon but are apparently unable to generate CO_2 within the carboxysome. *Plant Physiology*, **91**, 514–525.

Price, G.D., **Badger, M.R.** & **von Caemmerer, S.** (2011) The prospect of using cyanobacterial bicarbonate transporters to improve leaf photosynthesis in C3 crop plants. *Plant Physiology*, **155**, 20–26.

Price, G.D., **Badger, M.R.**, **Woodger, F.J.** & **Long, B.M.** (2008) Advances in understanding the cyanobacterial CO_2-concentrating-mechanism (CCM): functional components, Ci transporters, diversity, genetic regulation and prospects for engineering into plants. *Journal of Experimental Botany*, **59**, 1441–1461.

Price, G.D. & **Howitt, S.M.** (2014) Topology mapping to characterize cyanobacterial bicarbonate transporters: BicA (SulP/SLC26 family) and SbtA. *Molecular Membrane Biology*, **31**, 177–182.

Price, G.D., **Pengelly, J.J.L.**, **Forster, B.**, **Du, J.**, **Whitney, S.M.**, **von Caemmerer, S.** ***et al.*** (2013) The cyanobacterial CCM as a source of genes for improving photosynthetic CO_2 fixation in crop species. *Journal of Experimental Botany*, **64**, 753–768.

Price, G.D., **Woodger, F.J.**, **Badger, M.R.**, **Howitt, S.M.** & **Tucker, L.** (2004) Identification of a SulP-type bicarbonate transporter in marine cyanobacteria. *PNAS*, **101**, 18228–18233.

Prieß, M., **Göddeke, H.**, **Groenhof, G.** & **Schäfer, L.V.** (2018) Molecular mechanism of ATP hydrolysis in an ABC transporter. *ACS Central Science*, **4**, 1334–1343.

Pulsford, S.B., **Outram, M.A.**, **Förster, B.**, **Rhodes, T.**, **Williams, S.J.**, **Badger, M.R.** ***et al.*** (2024) Cyanobacterial α-carboxysome carbonic anhydrase is allosterically regulated by the rubisco substrate RuBP. *Science Advances*, **10**, 7283.

Qu, Z. & **Hartzell, H.C.** (2008) Bestrophin Cl channels are highly permeable to HCO_3^-. *American Journal of Physiology. Cell Physiology*, **294**, 1371–1377.

Rae, B.D., **Long, B.M.**, **Badger, M.R.** & **Price, G.D.** (2013) Functions, compositions, and evolution of the two types of carboxysomes: polyhedral microcompartments that facilitate CO_2 fixation in cyanobacteria and some proteobacteria. *Microbiology and Molecular Biology Reviews*, **77**, 357–379.

Raven, J.A., **Beardall, J.** & **Sánchez-Baracaldo, P.** (2017) The possible evolution and future of CO_2-concentrating mechanisms. *Journal of Experimental Botany*, **68**, 3701–3716.

Raza, S., **Sarkar, D.**, **Chan, L.J.G.**, **Mae, J.**, **Sutter, M.**, **Petzold, C.J.** ***et al.*** (2024) Comparative pore structure and dynamics for bacterial microcompartment shell protein assemblies in sheets or shells. *ACS Omega*, **9**, 35503–35514.

Reiskind, J.B., **Madsen, T.V.**, **Van Ginkel, L.C.** & **Bowes, G.** (1997) Evidence that inducible C4-type photosynthesis is a chloroplastic CO_2-concentrating mechanism in *Hydrilla*, a submersed monocot. *Plant, Cell & Environment*, **20**, 211–220.

Robison, T.A., **Oh, Z.G.**, **Lafferty, D.**, **Xu, X.**, **Villarreal, J.C.A.**, **Gunn, L.H.** ***et al.*** (2025) Hornworts reveal a spatial model for pyrenoid-based CO_2-concentrating mechanisms in land plants. *Nature Plants*, **11**, 63–73.

Rottet, S., **Rourke, L.M.**, **Pabuayon, I.C.M.**, **Phua, S.Y.**, **Yee, S.**, **Weerasooriya, H.N.** ***et al.*** (2024) Engineering the cyanobacterial ATP-driven BCT1 bicarbonate transporter for functional targeting to C3 plant chloroplasts. *bioRxiv*. Available from: https://doi.org/10.1101/2024.02.14.580295

Ryan, P., **Forrester, T.J.B.**, **Wroblewski, C.**, **Kenney, T.M.G.**, **Kitova, E.N.**, **Klassen, J.S.** ***et al.*** (2019) The small RbcS-like domains of the β-carboxysome structural protein CcmM bind RubisCO at a site distinct from that binding the RbcS subunit. *Journal of Biological Chemistry*, **294**, 2593–2603.

Sager, R. & **Palade, G.E.** (1957) Structure and development of the chloroplast in *Chlamydomonas* I. The normal green cell. *Journal of Biophysics and Biochemistry*, **3**, 463–488.

Sánchez-Baracaldo, P. (2015) Origin of marine planktonic cyanobacteria. *Scientific Reports*, **5**, 17418.

Sánchez-Baracaldo, P., **Ridgwell, A.** & **Raven, J.A.** (2014) A neoproterozoic transition in the marine nitrogen cycle. *Current Biology*, **24**, 652–657.

Sandrini, G., **Matthijs, H.C.P.**, **Verspagen, J.M.H.**, **Muyzer, G.** & **Huisman, J.** (2014) Genetic diversity of inorganic carbon uptake systems causes variation in CO_2 response of the cyanobacterium *Microcystis*. *ISME Journal*, **8**, 589–600.

Sarkar, D.I., **Maffeo, C.I.**, **Sutter, M.**, **Aksimentiev, A.**, **Kerfeld, C.A.**, **Vermaas, J.V.** ***et al.*** (2024) Atomic view of photosynthetic metabolite permeability pathways and confinement in synthetic carboxysome shells. *PNAS*, **121**, e2402277121.

Schirrmeister, B.E., **Gugger, M.** & **Donoghue, P.C.J.** (2015) Cyanobacteria and the great oxidation event: evidence from genes and fossils. *Palaeontology*, **58**, 769–785.

Schirrmeister, B.E., **Sanchez-Baracaldo, P.** & **Wacey, D.** (2016) Cyanobacterial evolution during the Precambrian. *International Journal of Astrobiology*, **15**, 187–204.

Selim, K.A., **Haase, F.**, **Hartmann, M.D.**, **Hagemann, M.** & **Forchhammer, K.** (2018) PII-like signaling protein SbtB links cAMP sensing with cyanobacterial inorganic carbon response. *Proceedings of the National Academy of Sciences of the United States of America*, **115**, E4861–E4869.

Shibata, M., **Katoh, H.**, **Sonoda, M.**, **Ohkawa, H.**, **Shimoyama, M.**, **Fukuzawa, H.** ***et al.*** (2002) Genes essential to sodium-dependent bicarbonate transport in cyanobacteria: function and phylogenetic analysis. *Journal of Biological Chemistry*, **277**, 18658–18664.

Shibata, M., **Ohkawa, H.**, **Kaneko, T.**, **Fukuzawa, H.**, **Tabata, S.**, **Kaplan, A.** ***et al.*** (2001) Distinct constitutive and low- CO_2-induced CO_2 uptake systems in cyanobacteria: genes involved and their phylogenetic relationship with homologous genes in other organisms. *PNAS*, **98**, 11789–11794.

Shimakawa, G., **Demulder, M.**, **Flori, S.**, **Kawamoto, A.**, **Tsuji, Y.**, **Nawaly, H.** ***et al.*** (2024) Diatom pyrenoids are encased in a protein shell that enables efficient CO_2 fixation. *Cell*, **187**, 5919–5934.

Shively, J.M., **Ball, F.**, **Brown, D.H.** & **Saunders, R.E.** (1973) Functional organelles in prokaryotes: polyhedral inclusions (carboxysomes) of *Thiobacllus neapolitanus*. *Science*, **182**, 584–586.

Shively, J.M., **Ball, F.L.** & **Kline, B.W.** (1973) Electron microscopy of the carboxysomes (polyhedral bodies) of *Thiobacillus neapolitanus*. *Journal of Bacteriology*, **116**, 1405–1411.

Sinetova, M.A., **Kupriyanova, E.V.**, **Markelova, A.G.**, **Allakhverdiev, S.I.** & **Pronina, N.A.** (2012) Identification and functional role of the carbonic anhydrase Cah3 in thylakoid membranes of pyrenoid of *Chlamydomonas reinhardtii*. *Biochimica et Biophysica Acta - Bioenergetics*, **1817**, 1248–1255.

So, A.K.C., **Espie, G.S.**, **Williams, E.B.**, **Shively, J.M.**, **Heinhorst, S.** & **Cannon, G.C.** (2004) A novel evolutionary lineage of carbonic anhydrase (ε class) is a component of the carboxysome shell. *Journal of Bacteriology*, **186**, 623–630.

Sommer, M., **Cai, F.**, **Melnicki, M.** & **Kerfeld, C.A.** (2017) β-Carboxysome bioinformatics: identification and evolution of new bacterial microcompartment protein gene classes and core locus constraints. *Journal of Experimental Botany*, **68**, 3841–3855.

© 2026 The Author(s).

Sun, H., **Cui, N.**, **Han, S.J.**, **Chen, Z.P.**, **Xia, L.Y.**, **Chen, Y. *et al.*** (2021) Complex structure reveals CcmM and CcmN form a heterotrimeric adaptor in β-carboxysome. *Protein Science*, **30**, 1566–1576.

Sun, Y., **Chen, T.**, **Ge, X.**, **Ni, T.**, **Dykes, G.F.**, **Zhang, P. *et al.*** (2025) Engineering CO_2-fixing modules in *Escherichia coli* via efficient assembly of cyanobacterial rubisco and carboxysomes. *Plant Communications*, **6**, 101217.

Sun, Y., **Harman, V.M.**, **Johnson, J.R.**, **Brownridge, P.J.**, **Chen, T.**, **Dykes, G.F. *et al.*** (2022) Decoding the absolute stoichiometric composition and structural plasticity of α-carboxysomes. *mBio*, **13**, e03629-21.

Sun, Y., **Sheng, Y.**, **Ni, T.**, **Ge, X.**, **Sarsby, J.**, **Brownridge, P.J. *et al.*** (2025) Rubisco packaging and stoichiometric composition of the native β-carboxysome in *Synechococcus elongatus* PCC7942. *Plant Physiology*, **197**, kiae665.

Sutter, M., **Laughlin, T.G.**, **Sloan, N.B.**, **Serwas, D.**, **Davies, K.M.** & **Kerfeld, C.A.** (2019) Structure of a synthetic β-carboxysome shell. *Plant Physiology*, **181**, 1050–1058.

Sutter, M., **Melnicki, M.R.**, **Schulz, F.**, **Woyke, T.** & **Kerfeld, C.A.** (2021) A catalog of the diversity and ubiquity of bacterial microcompartments. *Nature Communications*, **12**, 3809.

Tanaka, S., **Kerfeld, C.A.**, **Sawaya, M.R.**, **Cai, F.**, **Heinhorst, S.**, **Cannon, G.C. *et al.*** (2008) Atomic-level models of the bacterial carboxysome shell. *New Series*, **22**, 1083–1086.

Toyokawa, C., **Yamano, T.** & **Fukuzawa, H.** (2020) Pyrenoid starch sheath is required for LCIB localization and the CO_2-concentrating mechanism in green algae. *Plant Physiology*, **182**, 1883–1893.

Trettel, D.S., **Hoang, Y.**, **Vecchiarelli, A.G.** & **Gonzalez-Esquer, C.R.** (2025) Robust synthetic biology toolkit to advance carboxysome study and redesign. *ACS Synthetic Biology*, **14**, 2219–2229.

Trettel, D.S., **Neale, C.**, **Zhao, M.**, **Gnanakaran, S.** & **Gonzalez-Esquer, C.R.** (2023) Monatomic ions influence substrate permeation across bacterial microcompartment shells. *Scientific Reports*, **13**, 15738.

Treves, H., **Raanan, H.**, **Kedem, I.**, **Murik, O.**, **Keren, N.**, **Zer, H. *et al.*** (2016) The mechanisms whereby the green alga *Chlorella ohadii*, isolated from desert soil crust, exhibits unparalleled photodamage resistance. *New Phytologist*, **210**, 1229–1243.

Turnšek, J.B., **Oltrogge, L.M.** & **Savage, D.F.** (2024) Conserved and repetitive motifs in an intrinsically disordered protein drive α-carboxysome assembly. *Journal of Biological Chemistry*, **300**, 107532.

Villarreal, J.C. & **Renner, S.S.** (2012) Hornwort pyrenoids, carbon-concentrating structures, evolved and were lost at least five times during the last 100 million years. *Proceedings of the National Academy of Sciences of the United States of America*, **109**, 18873–18878.

Wang, C., **Sun, B.**, **Zhang, X.**, **Huang, X.**, **Zhang, M.**, **Guo, H. *et al.*** (2019) Structural mechanism of the active bicarbonate transporter from cyanobacteria. *Nature Plants*, **5**, 1184–1193.

Wang, P., **Li, J.**, **Li, T.**, **Li, K.**, **Ng, P.C.**, **Wang, S. *et al.*** (2024) Molecular principles of the assembly and construction of a carboxysome shell. *Science Advances*, **10**, eadr4227. Available from: https://doi.org/10.1126/sciadv.adr4227

Wang, Y. & **Spalding, M.H.** (2014) Acclimation to very low CO_2: contribution of limiting CO_2 inducible proteins, LCIB and LCIA, to inorganic carbon uptake in *Chlamydomonas reinhardtii*. *Plant Physiology*, **166**, 2040–2050.

Whitehead, L., **Long, B.M.**, **Dean Price, G.** & **Badger, M.R.** (2014) Comparing the in vivo function of α-carboxysomes and β-carboxysomes in two model cyanobacteria. *Plant Physiology*, **165**, 398–411.

Wieschollek, J., **Fuller, D.**, **Gahramanova, A.**, **Millen, T.**, **Mislay, A.J.**, **Payne, R.R. *et al.*** (2024) A new type of carboxysomal carbonic anhydrase in sulfur chemolithoautotrophs from alkaline environments. *Applied and Environmental Microbiology*, **90**, e0107524.

Wunder, T., **Cheng, S.L.H.**, **Lai, S.K.**, **Li, H.Y.** & **Mueller-Cajar, O.** (2018) The phase separation underlying the pyrenoid-based microalgal rubisco supercharger. *Nature Communications*, **9**, 5076.

Xu, J., **Fan, X.**, **Zhang, X.**, **Xu, D.**, **Mou, S.**, **Cao, S. *et al.*** (2012) Evidence of coexistence of C3 and C4 photosynthetic pathways in a green-tide-forming alga, *Ulva prolifera*. *PLoS One*, **7**, e37438.

Yadav, S., **Kalita, S.** & **Dubey, K.D.** (2024) Mechanism of a novel metal-free carbonic anhydrase. *Physical Chemistry Chemical Physics*, **26**, 28124–28132.

Yamano, T., **Sato, E.**, **Iguchi, H.**, **Fukuda, Y.** & **Fukuzawa, H.** (2015) Characterization of cooperative bicarbonate uptake into chloroplast stroma in the green alga *Chlamydomonas reinhardtii*. *Proceedings of the National Academy of Sciences of the United States of America*, **112**, 7315–7320.

Young, E.J., **Kirst, H.**, **Dwyer, M.E.**, **Vermaas, J.V.** & **Kerfeld, C.A.** (2025) Quantitative measurement of molecular permeability to a synthetic bacterial microcompartment shell system. *ACS Synthetic Biology*, **14**, 1405–1413.

Zang, K., **Wang, H.**, **Hartl, F.U.** & **Hayer-Hartl, M.** (2021) Scaffolding protein CcmM directs multiprotein phase separation in β-carboxysome biogenesis. *Nature Structural & Molecular Biology*, **28**, 909–922.

Zhan, Y., **Marchand, C.H.**, **Maes, A.**, **Mauries, A.**, **Sun, Y.**, **Dhaliwal, J.S. *et al.*** (2018) Pyrenoid functions revealed by proteomics in *Chlamydomonas reinhardtii*. *PLoS One*, **13**, e0185039.

Zhang, X., **Gao, G.**, **Gao, Z.**, **Gao, K.** & **Liu, D.** (2025) The contribution of biophysical and biochemical CO_2 concentration mechanisms to the carbon fixation of the green macroalga *Ulva prolifera*. *Marine Life Science & Technology*, **7**, 537–548.

Zhou, H., **Helliker, B.R.**, **Huber, M.**, **Dicks, A.** & **Akçay, E.** (2018) C4 photosynthesis and climate through the lens of optimality. *PNAS*, **115**, 12057–12062.

© 2026 The Author(s).